

March 2015

**Distribution and Transport of Pyrogenic Black Carbon in Soils  
Affected by Wildfires, Valles Caldera, New Mexico, with Implications  
for Contaminant Transport**

---

**WRRRI Technical Completion Report No. 365**

**Daniel Cadol  
Amy Galanter  
Phoebe Nicholls**



Redondito Peak following the Thompson Ridge Fire. Photo by Amy Galanter

**NEW MEXICO WATER RESOURCES RESEARCH INSTITUTE**  
New Mexico State University  
MSC 3167, PO Box 30001  
Las Cruces, New Mexico 88003-0001  
(575) 646-4337 email: [nmwrrri@wrrri.nmsu.edu](mailto:nmwrrri@wrrri.nmsu.edu)



DISTRIBUTION AND TRANSPORT OF PYROGENIC BLACK CARBON IN SOILS  
AFFECTED BY WILDFIRES, VALLES CALDERA, NEW MEXICO, WITH IMPLICATIONS  
FOR CONTAMINANT TRANSPORT

By

Daniel Cadol, Assistant Professor  
Amy Galanter, Graduate Assistant  
Phoebe Nicholls, Graduate Assistant  
Department of Earth and Environmental Science  
New Mexico Institute of Mining and Technology

TECHNICAL COMPLETION REPORT  
Account Number 118598

March, 2015

New Mexico Water Resources Research Institute  
in cooperation with the  
Department of Earth and Environmental Science  
New Mexico Institute of Mining and Technology

The research on which this report is based was financed in part by the U.S. Department of the Interior, Geological Survey, through the New Mexico Water Resources Research Institute.

## DISCLAIMER

The purpose of the Water Resources Research Institute (WRRI) technical reports is to provide a timely outlet for research results obtained on projects supported in whole or in part by the institute. Through these reports the WRRI promotes the free exchange of information and ideas and hopes to stimulate thoughtful discussions and actions that may lead to resolution of water problems. The WRRI, through peer review of draft reports, attempts to substantiate the accuracy of information contained within its reports, but the views expressed are those of the authors and do not necessarily reflect those of the WRRI or its reviewers. Contents of this publication do not necessarily reflect the views and policies of the Department of the Interior, nor does the mention of trade names or commercial products constitute their endorsement by the United States government.

## ABSTRACT

Wildland fires produce pyrogenic black carbon (PyC) on a continuum from soot to char. Post-fire runoff floods and debris flows subsequently transport and redeposit this material throughout the watershed. Our aim was to identify geomorphic settings where PyC accumulates and to study its impact on contaminant transport. Based on the capabilities of our PyC quantification method, this report focuses on the distribution of black carbon that combusts between 340-950°C, which includes most soot and some char. Sorption analyses utilized field soil samples in which the PyC was quantified in this combustion range, as well as soils that were augmented with char collected from the field site. This report presents the results of three related analyses: 1) a post-fire soils sampling effort, 2) a pre- and post-fire soil PyC content comparison, and 3) an analysis of the ability of soils with varying PyC contents to sorb arsenic from solution.

In the first study, three sites were sampled near Valles Caldera, NM: Thompson Ridge fire (TR; burned in 2013), Las Conchas fire (burned in 2011), and Cebolla Creek (control, unburned for >70 years). Sampling was stratified by geomorphic feature: floodplain, alluvial fan, and north- and south-facing hillslopes. Sites were sampled before and after the 2013 monsoon. Soot content as a fraction of total organic carbon decreased with time after the burn event, both for whole watersheds and for specific geomorphic settings. Floodplain soot content downstream of TR was higher than the other sites where recent flood evidence was observed, but lower beyond the limit of flooding. Soot content on floodplains downstream of both fires increased during the monsoon where flooding occurred. Hillslope soot redistribution on the north-facing TR hillslope during monsoon season showed decreases on the upper slope and increases near the toe of the slope, consistent with downslope transport by runoff. Other hillslopes analyzed did not show this movement. From this analysis, we conclude that soot is relatively mobile, and is predominantly transported by runoff and floods over short time scales following fire.

In the second study, soil samples that were collected at various locations on Redondo Peak in 2009 were obtained from a collaborator. We resampled the soil within 10 m of these locations in 2014. All sampling sites were within the burn perimeter of the Thompson Ridge fire, predominantly in moderate- to low-severity burn areas. The upper 5 cm of soil showed greater PyC content change between the two sampling times, while the soil between 5-15 cm depth was relatively stable in PyC content. Upslope locations tended to have reduced PyC concentrations in the post-fire sampling, while downslope locations tended to have increased PyC concentrations. We again attribute this to erosion and deposition of material by post-fire monsoon events that initiated overland flow.

In the final study presented here, field soils were mixed with sodium arsenate solutions varying from 0.001 to 0.1 mg/L. The low concentration solutions increased in As content over time, presumably as As was leached from the soil. The higher concentration solutions lost As through time, presumably via sorption onto the solids. Soils with added PyC content sorbed As more rapidly than the unchanged field soil samples, but all soils reached roughly the same equilibrium concentration. This suggests that PyC may be important in sorbing out heavy metals from mobile plumes, but is unlikely to change the long-term capacity of these soils to sequester heavy metals. Ongoing work with polycyclic aromatic hydrocarbons will evaluate whether this conclusion also holds for organic contaminants.

Key words:

pyrogenic black carbon, soil carbon, carbon cycle, erosion, sedimentation, soot

## TABLE OF CONTENTS

DISCLAIMER.....	ii
ABSTRACT.....	iii
TABLE OF CONTENTS.....	iv
LIST OF TABLES .....	v
LIST OF FIGURES .....	v
1. INTRODUCTION .....	1
1.1 OBJECTIVES AND SCOPE .....	1
1.2 STUDY AREA .....	1
1.3 BACKGROUND INFORMATION .....	3
2. METHODS .....	5
2.1 FIELD SAMPLING .....	5
2.1.1 GEOMORPHICALLY STRATIFIED SAMPLING.....	5
2.1.2 RESAMPLING OF ARCHIVED PRE-FIRE SOIL PITS .....	7
2.2 LABORATORY PyC ANALYSIS .....	8
2.3 ARSENIC SORPTION ANALYSIS .....	11
3. RESULTS .....	12
3.1 STANDARDS AND METHOD EVALUATION .....	12
3.2 BROAD SCALE SOIL BLACK CARBON DISTRIBUTION .....	13
3.3 PRE- AND POST-FIRE SOIL BLACK CARBON CONTENT .....	18
3.4 SORPTION OF ARSENIC ONTO SOILS AND BLACK CARBON .....	21
4. DISCUSSION .....	26
4.1 BLACK CARBON DISTRIBUTION .....	26
4.2 BLACK CARBON GENERATION AND RETENTION .....	27
4.3 BLACK CARBON TRANSPORT .....	28
4.4 POST-FIRE DEBRIS MANAGEMENT IMPLICATIONS .....	29
4.5 POTENTIAL TO SEQUESTER ARSENIC .....	29
4.6 ONGOING AND FUTURE WORK .....	30
REFERENCES .....	31

## LIST OF TABLES

Table 1. Results of analyses of kaolin, char, and bark standards.....	13
Table 2. Mean carbon stocks and ratios in pre- and post- fire soil pits.....	19

## LIST OF FIGURES

Figure 1. Broad-scale sampling points (yellow) for the three areas of the Jemez Mountains in and near Valles Caldera studied. The control watershed is Cebolla Creek; the burn perimeter labeled 2011 shows the Las Conchas fire and the burn perimeter labeled 2013 shows the Thompson Ridge fire.....	2
Figure 2. Map of soil textures in study area. Data extracted from the Natural Resources Conservation Service (NRCS) Soil Survey Geographic (SSURGO) database. ....	6
Figure 3. Locations of pre- and post-fire soil pit sampling sites. The map area is limited to the 2013 Thompson Ridge burn perimeter. Not all sampled sites have been analyzed, as shown in the legend. Some sites that were initially sampled did not have adequate archived soil volumes remaining, while others are still being analyzed.....	7
Figure 4. Pyrogenic black carbon content of soils collected in the 3 sampling areas. All geomorphic settings and sampling periods are included.....	14
Figure 5. PyC soil content site comparison stratified by geomorphic setting. See field methods for setting descriptions. Both pre- and post-monsoon data are included. ....	15
Figure 6. PyC soil content of alluvial fan sites stratified by longitudinal position on the fan. Only pre-monsoon data have been analyzed.....	15
Figure 7. PyC soil content of floodplain sites stratified by distance from bank. Both pre- and post-monsoon data are included.....	16
Figure 8. PyC soil content of north-facing hillslope sites stratified by longitudinal position on the hillslope. Both pre- and post-monsoon data are included.....	16
Figure 9. PyC soil content of south-facing hillslope sites stratified by longitudinal position on the hillslope. Both pre- and post-monsoon data are included.....	16
Figure 10. PyC soil content of the north- and south-facing hillslope sites in the Thompson Ridge burn area stratified by longitudinal position on the hillslope. July sample period was prior to most of the monsoon precipitation in 2013, while the September sample period followed the monsoon season.....	17
Figure 11. PyC soil content of the floodplain site, stratified by distance from the bank, in A) the Thompson Ridge burn area, and B) the Las Conchas burn area. July sample period was prior to most of the monsoon precipitation in 2013, while the September sample period followed the monsoon season. Sample sizes are $n = 2$ for each box. ....	17

Figure 12. Pyrogenic black carbon (PyC) content as a fraction of total organic carbon (TOC) in soil samples from the Thompson Ridge burn taken before (2009) and after (2014) the fire. The “O” horizon was the upper 5 cm of soil if horizonation was not distinguishable following the fire.....	18
Figure 13. Temporal change in the ratio of pyrogenic black carbon to total organic carbon in soil pit samples. Points close to the 1:1 line were relatively unchanged in the Thompson Ridge fire. Point above the line gained black carbon, while points below the line lost black carbon.....	19
Figure 14. Temporal change in the pyrogenic black carbon content and the total organic carbon content in soil pit samples. Values are mass of PyC per unit mass of analyzed soil and mass of TOC per unit mass of soil. Soils were ground and sieved before analysis, removing any clasts larger than 250 $\mu\text{m}$ .....	19
Figure 15. PyC/TOC ratio values of all analyzed sites, split by watershed group and soil horizon, then sorted into upslope (near the drainage divide) to downslope (near the watershed outlet) order. Blue circles are the 2009 data and red squares are the 2014 data. Note the relative stability of the A horizon samples. In some watersheds, the O horizon data show a trend toward PyC loss in the upslope areas and PyC gain in the downslope areas. Watershed group numbers correspond to numbers on the sample location map (Figure 3). Not all sampling locations had both O and A horizon data, or both 2009 and 2014 data, resulting in data gaps. ....	20
Figure 16. Sorption kinetics for 0.001 mg/L As solution.....	22
Figure 17. Sorption kinetics for 0.005 mg/L As solution.....	22
Figure 18. Sorption kinetics for 0.01 mg/L As solution.....	23
Figure 19. Sorption kinetics for 0.1 mg/L As solution.....	23
Figure 20. Sorption kinetics on the floodplain soil for all 4 As solutions.....	23
Figure 21. Equilibrium isotherms for arsenic sorption to the floodplain and hillslope soils. The left figure has a linear scale, while the right figure has a logarithmic scale...	24
Figure 22. ORP and pH data of equilibrated sorbent-sorbate systems plotted on an Eh-pH diagram for the As-H <sub>2</sub> O system, from Masscheleyn et al. 1991. Activities of As, Mn, and Fe were all taken to be 10 <sup>-4</sup> . Species areas indicated are ‘predominance areas’, not strict limits for existence. ....	25
Figure 23. Same Eh-pH diagram as Figure 21, from Masscheleyn et al. 1991, with sample pH and ORP separated according to the concentration of As sorbate solution. ....	26

# 1. INTRODUCTION

## 1.1 Objectives and Scope

The objectives of this research were to 1) identify the relative importance of mass movement and river flow in transporting pyrogenic black carbon (PyC) through recently burned semi-arid watersheds, 2) identify geomorphic contexts where PyC accumulates, and 3) assess the potential of PyC deposits to sequester contaminants.

We conducted two separate field sampling campaigns to address the first two objectives. The first was a broad post-fire random sampling that was stratified by geomorphic feature, while the second took advantage of archived 2009 soil samples from the area burned by the Thompson Ridge fire in 2013. This took advantage of a serendipitous connection with collaborator Kathleen Lohse, of Idaho State University. In these analyses, we predominantly quantify the soot portion of the PyC spectrum in the study site. This is due to a weakness in the Chemothermal Oxidation (CTO) method which was used: some char may be combusted in the process of removing organic carbon via combustion at 340 or 375 °C. The use of the benzene polycarboxylic acid (BPCA) quantification method, which has the potential to quantify both soot and char (Dittmar, 2008), is also being explored for future work (see Methods Section 2.2 below). The third objective was addressed by conducting batch equilibrium sorption tests, with arsenic as the sorbate. This heavy metal is naturally present in the study watershed and is significant from a water quality perspective. It is anticipated that future work will also test sorption of an aromatic hydrocarbon such as benzene as a representative organic contaminant.

## 1.2 Study Area

To accomplish these objectives, soils samples from two recently burned areas and a control watershed in the Jemez Mountains of New Mexico were collected and analyzed for black carbon. The study site selection process was modified early in the project to take advantage of the occurrence of the Thompson Ridge fire in Valles Caldera National Preserve in June 2013. Rather than sampling from fires across the state, as initially planned, we sampled geomorphic features affected by the Thompson Ridge fire (2013), the Las Conchas fire (2011), and in Cebolla Creek



watershed, which has not experienced a major burn in the past 70 years (Figure 1). In the early summer of 2011, the Las Conchas fire burned 156,593 acres, including a large area of the Valles Caldera National Preserve (SWCC, 2012). Two years later in May 2013, the Thompson Ridge fire ignited and burned 23,965 acres in the Valles Caldera National Preserve (IIS, 2013). Located in the Southern Rockies ecoregion, the Valles Caldera is well-studied by a broad range of earth scientists, in part due to its clearly preserved volcanic caldera morphology and in part due to its land management practices, which promote scientific research. It is a National Preserve, in the process of being transferred to National Park Service management, as well as part of the Critical Zone Observatory (CZO) network (Chorover et al., 2011). With a diameter of 20 km, the central valley hosts prairie grasses and meandering streams. The mountains and hills formed by the walls and the resurgent and extrusive domes of the caldera are vegetated by ponderosa pines, aspens, and grasses.

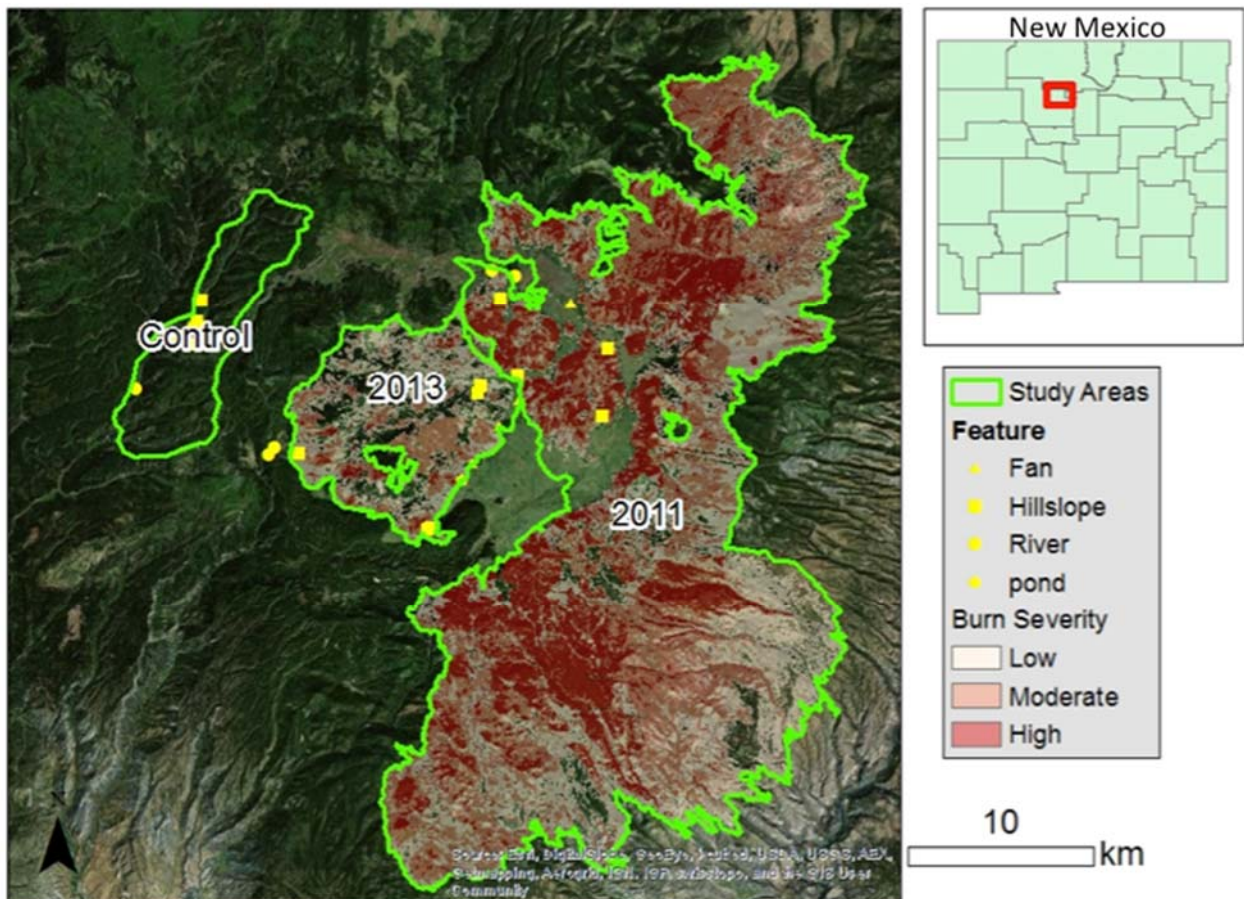


Figure 1. Broad-scale sampling points (yellow) for the three areas of the Jemez Mountains in and near Valles Caldera studied. The control watershed is Cebolla Creek. The burn perimeter labeled 2011 shows the Las Conchas fire and the burn perimeter labeled 2013 shows the Thompson Ridge fire.

### 1.3 Background Information

The severity and frequency of forest fires have increased since the 1980s in the American Southwest (Dillon et al., 2011) and are predicted to continue to increase as a result of past fire management strategies, climate change, and shifts in land use (Litschert et al., 2012). It is increasingly important to understand the effects of wildfire on water quality (Smith, 2011). Black carbon (BC), the residue from partial combustion of organic matter, typically accounts for ~4% of total soil carbon, although this can vary greatly with fire regime and other factors (Cornelissen et al., 2005), and 9% of organic carbon in aquatic sediments (Koelmans et al., 2006). There are two principal forms of BC – soot, a graphitized condensate, and char, a solid residue (Schmidt and Noack, 2000). The range of forms of BC has been described as falling along a ‘combustion continuum’, which has led to some contradicting definitions and difficulties in comparing quantifications using different analytical techniques (Masiello, 2004). There are a variety of methods for measuring BC in soils (e.g., Kuhlbusch, 1995; Brodowski et al., 2005), which in combination with the variety of BC forms has led to some difficulty comparing work from various researchers. Fortunately, the research community has endeavored to systematically compare the various techniques (Hammes et al., 2007), and there is now some degree of translatability among them. The most commonly used method, and the one presented in this study, is chemo-thermal oxidation (CTO; see methods).

Soil BC has the potential to be an important component of the global carbon cycle because of its recalcitrant nature (Forbes et al., 2006). Although BC has a much higher refractory component than organic carbon and would therefore be expected to be extremely stable in the soil (Cheng et al., 2008; Liang et al., 2008) there is emerging evidence that the residence time of BC, while still on the order of centuries, is less than the previously predicted millennia (Hammes et al., 2008; Ohlson et al., 2009). This may be due to consumption of soil BC in subsequent fires (Certini, 2005), degradation of BC by microbes and fungi (Hockaday et al., 2006), or erosion and remobilization of the BC (Czimeczik et al., 2003; Eckmeier et al., 2007; Nguyen et al., 2008). Some degree of chemical degradation is supported by the discovery of BC-like material in river water (Kim et al., 2004; Jaffe et al., 2013), but the frequently proposed possibility of erosional removal has not been quantified.

A second potentially important aspect of BC is its ability to sequester contaminants (Koelmans et al., 2006). Polycyclic aromatic hydrocarbon (PAH) partitioning in soils appears to be dominantly controlled by BC (Accardi-Dey and Gschwend, 2003; Ghosh, 2007), likely due to the large specific surface area and abundant surface sites and nanopores (Cornelissen et al., 2005). The interactions among organic components and black carbon in actual sediment deposits, however, make generalizations very tenuous (Arp et al., 2009; Staniszewska et al., 2011). Black carbon is also frequently used as a sorbent in the removal of heavy metals, though sequestration potential appears to be soil or site specific. Black carbon has also been shown to effectively sorb lead (Qiu et al., 2008) and chromium (Wang et al., 2010), and has the potential to sorb significant quantities of other heavy metals (Bailey et al., 1999). Heavy metals can also alter BCs ability to sorb PAHs, particularly if the BC is in the form of char (Chen et al., 2007). Competitive sorption is an issue in any attempt to quantify the sorption characteristics of black carbon, as even the presence of simple salt ions in the solution may affect equilibrium concentrations.

A final potentially important aspect of BC is its role in soil nutrient retention and pedogenesis. Organic matter and BC both contribute to the retention of nutrient cations in soils (Lehmann, 2007), although BC contributes disproportionately to the retention of nutrients in soils, relative to organic carbon, because of its greater surface area, negative surface charge, and charge density (Liang et al., 2006). Additionally, BC appears to be able to retain phosphate, in spite of the negative charge on both components (Liang et al., 2006). The Anthrosols, or Terra Preta de Indio, of the Amazon basin, which appear to be large-scale soil amendment projects carried out by pre-Colombian inhabitants, are a striking example of the ability of BC to improve soil fertility (Lehmann et al., 2003). In boreal forests, wildfire derived charcoal increases nitrification, possibly by sorbing out naturally occurring chemical inhibitors of microbial activity (DeLuca et al., 2006), but interestingly the effect is primarily seen with char generated by wildfires and not with char generated in the laboratory (Gundale and DeLuca, 2007). Additionally, with the evidence for century-scale BC degradation, there is an emerging view that BC is not simply a passive, refractory contributor to soil carbon, but that it is an active and mobile contributor to pedogenesis (Czimczik and Masiello, 2007).

## 2 METHODS

### 2.1 Field Sampling

#### 2.1.1 Geomorphically stratified sampling

To accomplish the objectives at the landscape scale, soils samples from two recent burns and a control watershed in the Jemez Mountains were collected and analyzed for black carbon using the standard CTO-375 method. The sampling protocol was modified early in the study to take advantage of the occurrence of the Thompson Ridge fire in Valles Caldera National Preserve in June 2013. As designated in Figure 1, three sub-sites were selected for study. A Geographic Information System (GIS) was employed to compile data on topography, geomorphology, geology, channel networks, slope, aspect, and burn severity. Soil type was not controlled for (Figure 2). Sampling locations were selected by determining a set of combinations to target, and then employing a random point generation program to minimize site selection bias.

A total of eight features were selected for sampling in each of the three study sub-sites: 4 hillslopes, 2 alluvial fans, and 2 stream reaches. The 4 hillslopes were stratified by aspect (north vs. south facing) and by slope ( $>20^\circ$  vs.  $<20^\circ$ ). All were in high severity burn zones. Six samples were taken from each hillslope: 2 near the ridge, 2 at mid-slope, and 2 near the toe of the slope. In each site, as many alluvial fans as possible were identified from air photos and digital elevation models, and then 2 were randomly selected. Nine samples were taken from each fan: 3 near the apex, 3 at mid-fan, and 3 near the toe of the fan. Even with nine fan samples, it is likely that our sampling misses some of the variability of these complex depositional environments, which commonly exhibit debris flow, hyperconcentrated flow, as well as streamflow processes. All perennial streams in each study area were digitized and split into 500 m reaches, two of which were randomly selected. Three evenly spaced transects were sampled for each selected reach. At each transect 6 samples were collected: one each on either bank, one each 3 m away from either bank, and one each 12 m away from either bank. There were a total of 78 soil samples collected from each of the three sub-sites at each of two sampling periods. Soil samples were taken before the monsoon season of 2013 (during the month of July) and after the monsoon season of 2013 (during the month of September). Not all have yet been analyzed, but a representative sampling is presented in this report.



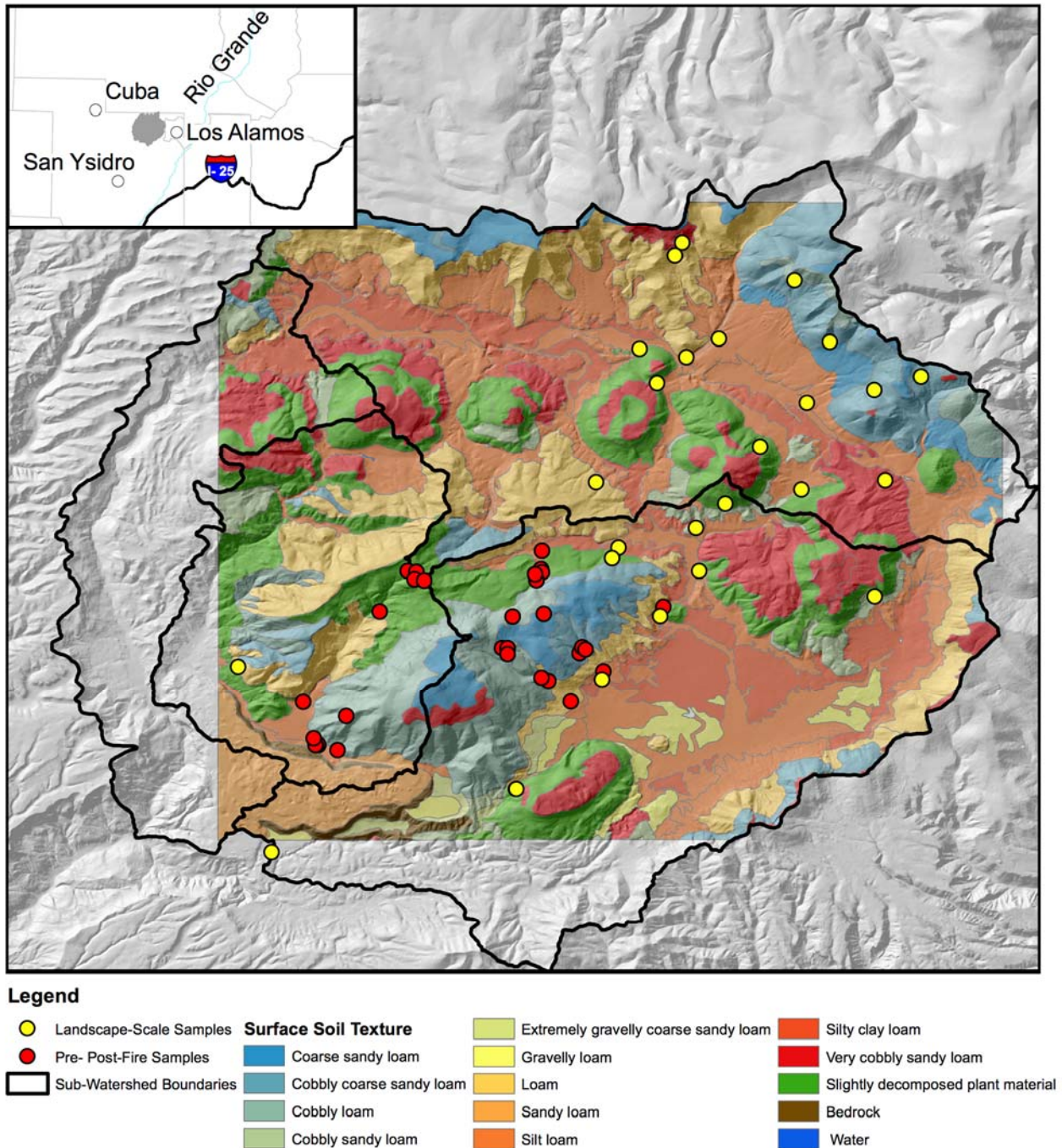


Figure 2. Map of soil textures in study area. Data extracted from the Natural Resources Conservation Service (NRCS) Soil Survey Geographic (SSURGO) database.

Soil samples were collected using a uniform protocol. For each soil sample, a small hole of roughly 15-20 centimeters in diameter and 15-20 centimeters in depth was excavated. Soil material was mixed before a sample was collected and stored in a foil container for transport back to the laboratory. Litter was rarely present, but if so, was included along with duff and ash.

Soils were typically sandy loams with generally high gravel and cobble contents on the hillslopes (Figure 2). Valley bottoms, though not extensively sampled in this study, tended to have finer compositions. Hillslopes with substantial litter at the time of the Natural Resources Conservation Service NRCS soil survey are indicated, though this particular soil unit (Origo map unit), which was present at several of our sites, was underlain by very cobbly sandy loam.

### 2.1.2 Resampling of archived pre-fire soil pits

In the summer of 2009, Kathleen Lohse and colleagues collected soil samples at a range of sites in the central region of Valles Caldera as part of initial CZO data compilation (Figure 3). Sites were stratified on forest type: ponderosa, mixed conifer, and aspen. Soil pits were dug and 10 cm by 10 cm samples of the O and A horizons were collected. The O horizon typically extended 5-7 cm below the soil surface and included the duff layer. Ash layers were not observed, but would have been included. Only the upper 10 cm of the A horizon was collected, meaning that a 10 cm cube of soil was collected. Soil pit locations were recorded with a basic handheld GPS receiver, with an estimated uncertainty of 10 m. Soil samples were kept on ice in the field, dried, and ground in the lab, subsampled for various nutrient analyses, and finally archived in a freezer.

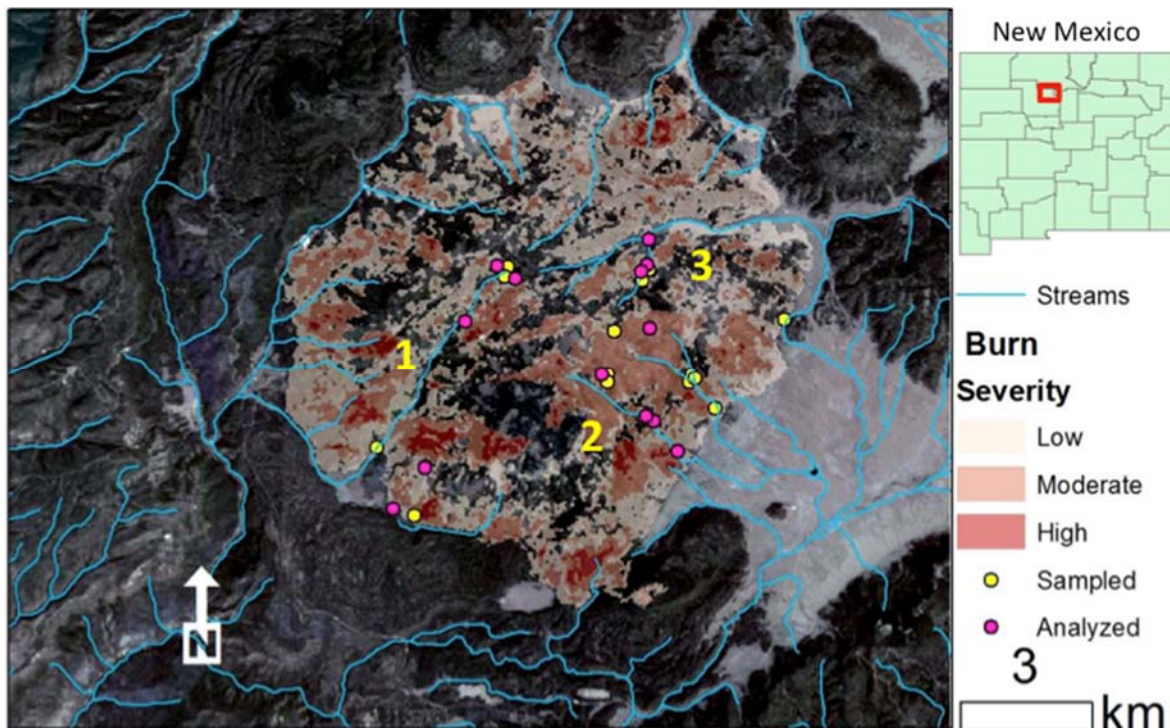


Figure 3. Locations of pre- and post-fire soil pit sampling sites. The map area is limited to the 2013 Thompson Ridge burn perimeter. Not all sampled sites have been analyzed. Some sites that were initially sampled did not have adequate archived soil volumes remaining, while others are still being analyzed.

In the summer of 2014, one year after the Thompson Ridge fire burned through most of the 2009 sample sites, the locations were resampled using the same protocol. The sites were relocated using a similar GPS receiver with similar estimated uncertainty, leading to a possible relocation error of up to 20 m. Soils horizons were not distinguishable in many of the resampled pits, in which case the upper 5 cm was sampled and identified as the “O” horizon, with the 5-15 cm depth interval being identified as the “A” horizon.

## **2.2 Laboratory PyC Analysis**

Soil samples were analyzed for labile organic carbon content (OC), inorganic carbon (IC) content, and pyrogenic black carbon (PyC) content. The methodology was adapted from standardized methods published as Chemo-Thermal Oxidation at 375°C (CTO-375), (Hammes et al., 2007, Nguyen et al., 2004, Gustaffson et al., 1997). The method quantifies black carbon as the carbon remaining after a sample is combusted at 375°C and acidified. The remainder is subsequently combusted at 900°C and any carbon evolved in this step is assumed to be PyC. We analyzed our broad-scale samples using this published procedure. The first combustion was performed using a high temperature furnace. The acidification and final combustion were performed using a Shimadzu total carbon analyzer (Shimadzu TOC SSM 5000a), an instrument made available to our research group by the Environmental Chemistry research group at New Mexico Tech. We tested the methodology with a series of standards: a soil standard that was tested for PyC by the University of Zurich, char collected from burned ponderosa pine logs at the field site, unburned ponderosa bark, kaolinite, and blanks. We used a streamlined modification of the procedure to analyze the pre- and post-fire soil pit samples, incorporating improvements described in subsequent publications from additional research groups (Kuhlbusch et al., 1995; Gustaffson et al., 1997; Nguyen et al., 2004; Elmquist et al., 2004; Caria et al., 2011).

Upon return from field sampling, all samples were dried at 60°C in a low temperature oven for 12-24 hours, depending on the moisture content of the soil. Samples were then ground with a mortar and pestle and sieved through a 250 µm mesh until ~250 mg of sample was prepared. Samples were deposited into pre-weighed ceramic boats, which were then weighed with the sample using an analytical scale. The broad-scale samples were then combusted in a 375°C oven in the presence of excess oxygen for 24 hours to remove non-BC organic carbon (OC). The

amount of OC combusted to form CO<sub>2</sub> was quantified as the mass difference before and after combustion.

The samples were then acidified to remove inorganic carbon (IC). For the broad-scale samples this was done in the Shimadzu soil sample module (SSM) using phosphoric acid and a 200°C furnace. The carbon dioxide produced in this step was measured using an infrared absorbance spectrum analyzer, with the signal reported in mV and measured at a 1 second time step. Area under the absorbance curve was calibrated to mass of carbon evolved using NaHCO<sub>3</sub> to develop a linear calibration curve.

The final combustion step evolved the organic carbon that was not previously released. The assumption is that black carbon is formed at high temperatures (>375°C) and will not react during the first combustion. This is only true for more condensed forms of PyC, therefore this protocol, called CTO-375, is best considered a measure of soot only. The sample was inserted into a high temperature furnace in the Shimadzu SSM that combusted the sample at 900°C. The carbon dioxide produced in this step was measured using the same infrared absorbance analyzer as in the IC step, calibrated using C<sub>8</sub>H<sub>5</sub>O<sub>4</sub>K to develop the mV absorbance to mg of C conversion factor.

In the analysis of the pre- and post-fire soil pit samples we removed the organic carbon (OC) by combustion at 340°C for 18 hours before acidification, acidified with 1 M HCl, and performed TOC analysis at 950°C, a protocol that will expand the range of PyC measured from the CTO-375 implementation described above. We assume that OC can be eliminated at temperatures of 340°C or less and that PyC endures beyond 340°C. Since black carbon is often defined as a continuum (Goldberg, 1985) we realize that significant PyC may be eliminated at temperatures below 340°C and that some PyC may persist at temperatures greater than 950°C. Despite these limitations, we are confident that the method we have developed is consistent, reliable, and capable of determining changes in PyC concentrations in watersheds impacted by wildfire.

The CTO method was largely developed to quantify highly condensed forms of black carbon (Gustaffson et al., 1997; Elmquist et al., 2004; Nguyen et al., 2004) by combusting PyC at 375°C



for 24 hours; this method does not quantify the full spectrum of PyC because low-condensed char is eliminated as OC (Hammes et al., 2007). By reducing the temperature and time of the oxidation, we are able to quantify more of the spectrum of PyC that is generated in a wildfire. Kuhlbusch et al. (1995) used a lower temperature of 340°C during the first elimination step based on thermal investigations that showed no significant production or destruction of PyC at 340°C. Kuhlbusch et al. (1995) used pure oxygen gas as the carrier gas and combusted the samples for 2 hours. We were unable to use pure oxygen gas for the first elimination step and instead combusted the samples in air for 18 hours. We selected 18 hours based on in-house optimization tests as well as kinetic studies of char combustion in air compared to char combustion in pure oxygen (Nguyen et al., 2004; Elmquist et al., 2004).

After the elimination of OC, we performed in-situ micro acidification with 1 M HCl. We performed the OC elimination first because acidification before combustion may lead to cake formation, which limits oxygen distribution in the sediment during the combustion step (Gustaffson, 1997; Elmquist 2004). Performing acidification first can also alter the thermal properties of the remaining organic carbon, potentially causing it to be measured as black carbon (Caria et al., 2011). We acidified each sample with aliquots of 250  $\mu$ L HCl until the sample was completely acidified and no longer produced effervescence. We then analyzed the samples in the total carbon analyzer for carbon evolved at 950°C, a slightly higher temperature than the 900°C used on the broad-scale samples. This permits a slight expansion of the range of the black carbon continuum measured.

Unless the carbon evolved in OC combustion is directly quantified, the CTO method is considered semi-quantitative (Schumacher, 2002). Some researchers determine the loss of OC gravimetrically (Gustaffson et al., 1997; Gustaffson et al., 2001) or by thermogravimetric analysis and differential thermal analysis (TGA/DTA) (Nguyen et al., 2004), although mass loss is not strictly equal to carbon loss. For our pre- and post-fire samples, we quantified the OC by performing a total organic carbon (TOC) analysis and a PyC analysis for each sample. For the TOC analysis, we completed the acidification and total carbon analysis and omitted the OC elimination, not distinguishing OC from PyC. For the PyC analysis, we performed the OC elimination, acidification, and total carbon analysis, making a clear distinction between OC and

PyC. In this way, we are able to estimate quantitatively the OC that was lost during the 18 hour combustion and we are able to report the PyC concentrations as a fraction of TOC, which is an accepted way of reporting black carbon data (Cornelissen et al., 2005). The potential for organic carbon to be digested in the acidification step introduces some error into the TOC estimate. However, in-house trials reversing step order and comparing OC mass loss during combustion conducted before or after acidification suggest that the introduced bias will be less than 5%.

An alternative method of quantifying PyC, the BPCA method, is being investigated for future implementation. This method is capable of analyzing the combined char and soot content of soil samples, that is, the full spectrum of pyrogenic black carbon (PyC), and can also measure the dissolved black carbon (DBC) content of water samples (Jaffe, 2013). The BPCA method assumes that PyC polymers can be broken down into BPCA monomers, which can then be analyzed via a High Performance Liquid Chromatograph (HPLC). Samples are acidified with nitric acid, which enables the breakdown of PyC into BPCA monomers. The solution of the sample containing nitric acid and converted BPCAs is purified via several filtration and extraction steps and finally transferred to HPLC vials in ultrapure water (Wiedemeier et al., 2013). Chromatographic BPCA separation is performed and the ultra-violet absorbance peaks are correlated to standards for the various BPCA species and molecular structures. The peaks are converted to individual concentrations then summed, giving a measure of total BPCA that is then converted back to total PyC.

### **2.3 Arsenic Sorption Analysis**

Soil was collected from a hill slope and a floodplain site in the Valles Caldera study area affected by the 2013 Thompson Ridge fire. Samples were taken following the first post-fire monsoon season. Soil was collected from a 50 cm diameter and 20 cm deep pit and placing the mixed soil in a plastic Ziploc bag. Pure black carbon samples were collected from charred trees. The soil was then taken back to the lab and dried at 105°C. It was sieved to 2 mm and split into 2-gram portions using a soil splitter. The black carbon was also dried at 105°C and sieved to 2 mm.

Four arsenic solutions were created with concentrations of 0.001 mg/L, 0.005 mg/L, 0.01 mg/L, and 0.1 mg/L by diluting a stock solution of 2 mg/L. Each solution was created by dissolving

sodium arsenate into a 1 M solution of sodium chloride. Sodium chloride was used to mimic natural cation exchange conditions between the soil and the solution.

To determine the time for the soil and solution to reach equilibrium, 70mL of each solution was added to each type of soil. Soil types include floodplain, hillslope, floodplain with added PyC, and pure PyC. The mixture of PyC and floodplain soil was a 4% PyC mixture by weight. The total mass of soil for each batch was 2 g. At each time step, 4 mL of solution was extracted to be analyzed by an ICP-MS. Extraction times were exponential and there were six extraction times for each reaction, ranging from 1 hour to 140 hours post-mixing.

An Agilent 7900 ICP-MS was used to measure trace metal concentrations. The internal standard for arsenic was germanium. The concentration of the solution at each time step was measured. The amount of arsenic sorbed was calculated by finding the amount of arsenic in solution at each time step and subtracting from the initial mass of arsenic in solution. The mass was then divided by the mass of the soil in order to determine the concentration of arsenic sorbed at each extraction time.

Three 50 mL replicates of each concentration and soil type were mixed in order to fit a sorption isotherm to the data. Each reaction was run to its full equilibrium time. Three isotherms were tested against the data: Freundlich, Langmuir, and Dubinin-Radushkevich. The quality of fit of the various equations permits us to speculate on the mechanism driving sorption.

### **3. RESULTS**

#### **3.1 Standards and Method Evaluation**

We analyzed the following standards to evaluate method performance: a soil standard that was tested for PyC by the University of Zurich using the CTO-375 method, black carbon (char) collected from the field site, unburned ponderosa pine bark, kaolin clay from a pottery supplier, and blanks. Our analysis of the standard was in moderately good agreement with the reported content, with < 8% overestimation of PyC content as a fraction of total organic carbon (TOC)

relative to the reported content. Blanks analyzed in the Shimadzu yielded PyC contents < 0.001 mg.

The field char, bark, and kaolin were valuable for method evaluation, and results are reported in Table 1. In analyzing the kaolin clay, we found that this method may either evolve carbon from clay minerals or the instrument may measure a small amounts of leaked carbon or CO<sub>2</sub> in the 900°C combustion step. The blank analyses also suggested a possibility of introduced carbon in this step, but the kaolin analyses gave an order of magnitude higher maximum PyC readings than the blank analyses.

In analyzing the char from the field, we noted that the CTO-375 method of PyC quantification almost completely combusts the char deposits characteristic of our field site in the 375°C organic combustion step (Table 1). Thus the method is only measuring the soot component of PyC at our field site.

The bark analysis found no PyC content, as expected, though it did measure more inorganic carbon than anticipated. We are less concerned about errors and uncertainties in IC measurement, since we report PyC as a fraction of TOC (i.e., OC plus PyC). If it were reported as a fraction of total carbon, this would be an issue, but we avoided this because of known differences in lithology at the three field sites and potential resultant variation in IC content.

Table 1. Results of analyses of kaolin, char, and bark standards

	# of analyses	OC (mg, ave.)	IC (mg, ave.)	PyC (mg, ave.)	PyC/(OC+PyC)
kaolin	4	1.73	0.016	0.049	0.0275
char	4	161.85	0.018	0.066	0.0004
bark	1	39.55	0.452	0.000	0.0000

### 3.2 Broad-scale Soil Black Carbon Distribution

The three sub-sites from which soil was collected were Cebolla Creek, the Las Conchas burn, and the Thompson Ridge burn (abbreviated C, LC, and TR in subsequent figures). Averaging across all geomorphic features sampled and both the pre- and post-monsoon sampling periods, median black carbon soot content (measured using the CTO-375 method), as a fraction of total

organic carbon, was highest in the Thompson Ridge burn, second highest in the Las Conchas burn, and lowest in the Cebolla Creek control (Figure 4). This trend is the inverse of the time since the last fire; TR burned 1-4 months prior to sampling, LC burned 2 years prior to sampling, and C burned >70 years prior to sampling. The two burned sampling areas are significantly different from the control at the 95% confidence level, but are not significantly different from each other ( $p = 0.91$ ) when analyzed with the Tukey honestly significant difference (HSD) test (found using R version 3.1.0).

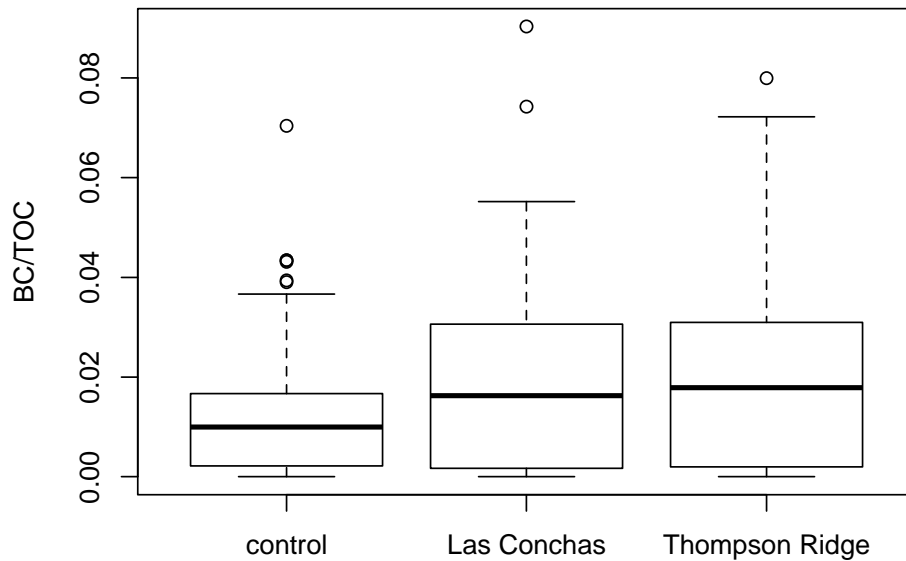


Figure 4: Pyrogenic black carbon content of soils collected in the 3 sampling areas. All geomorphic settings and sampling periods are included.

When analyzing the data by geomorphic feature, the same trend of increasing PyC content with decreasing time since burn continues (Figure 5). Fewer comparisons are significantly different at the 95% level, again using the Tukey HSD test: the TR fan data is different than the C and LC fan data; no floodplains are significantly different; the TR north-facing hillslope data is almost significantly different from the control ( $p = 0.06$ ); and no south-facing hillslopes are significantly different.

The alluvial fan samples were the least extensive data set, in that the post-monsoon samples have not been analyzed. The TR fan had significantly greater PyC content than either the control or LC burn area (Tukey HSD) at all sub-feature locations: high on the fan, in mid-fan, and at the toe of the fan (Figure 6).

The floodplain-sampling regime included samples taken at the stream bank, 3 m away from the bank, and 12 m away from the bank. The trend of increasing PyC content with decreasing time since burn continues for sites near the banks, but breaks down at the sampling sites farthest from the stream, 12 m away (Figure 7). The TR floodplain site showed evidence of flooding such as flattened grasses even prior to the pre-monsoon sample, but these indicators extended less than 12 m from the banks. TR was significantly different from the control at 3 m and 12 m from the bank, but this significance is influenced by the greater sample size for the control site. Five river transects were analyzed from Cebolla Creek, while only one transect from the two burn areas were analyzed. The north and south facing hillslope data generally continue the trend of increasing PyC content with decreasing time since burn at the sample site (Figures 8 & 9), but no PyC comparisons among the sites are significantly different (Tukey HSD).

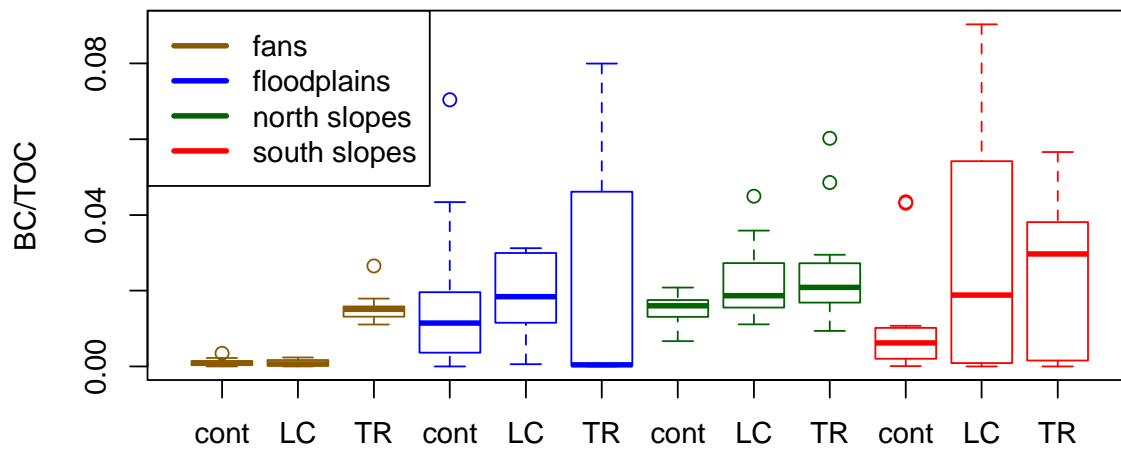


Figure 5. PyC soil content site comparison stratified by geomorphic setting. See field methods for setting descriptions. Both pre- and post-monsoon data are included in this plot.

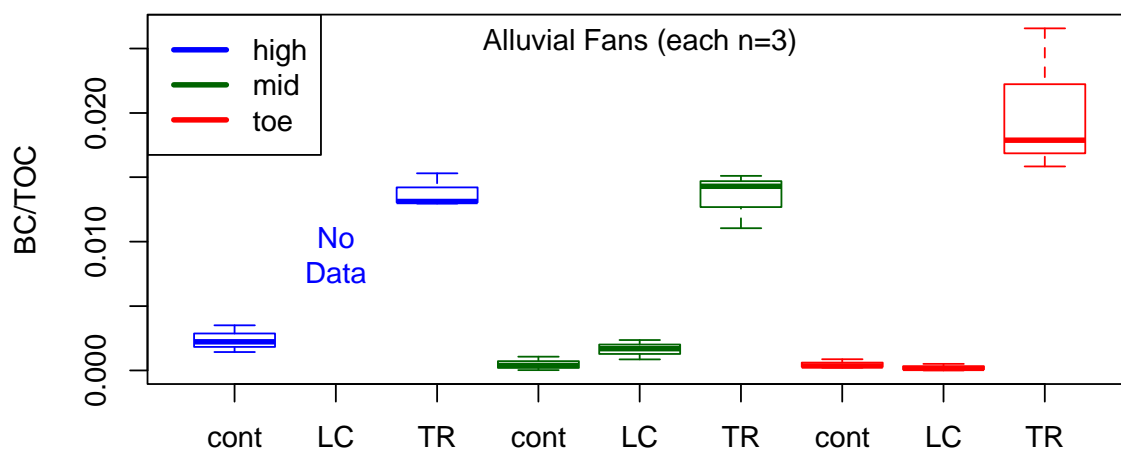


Figure 6. PyC soil content of alluvial fan sites stratified by longitudinal position on the fan. Only pre-monsoon data are included in this plot.

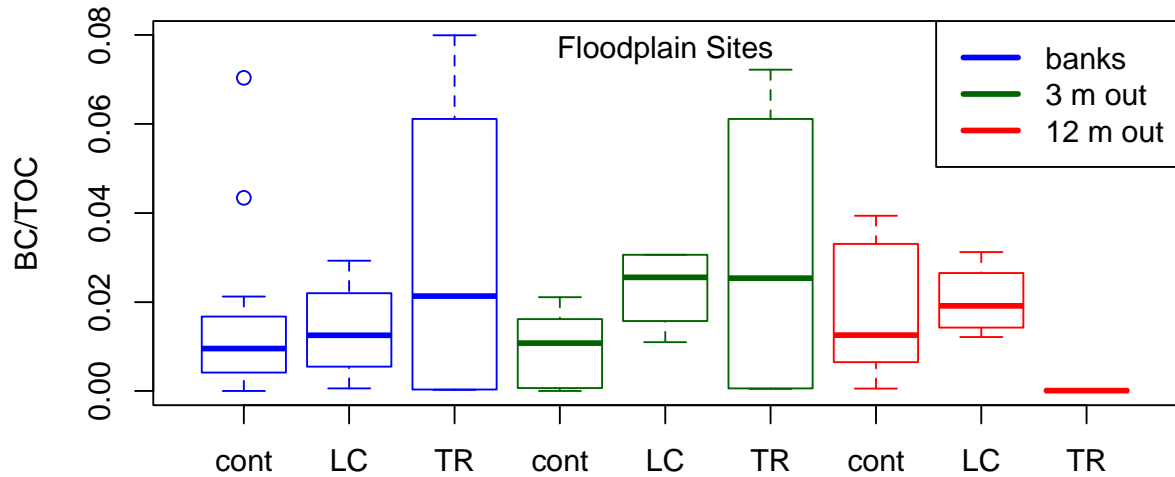


Figure 7. PyC soil content of floodplain sites stratified by distance from bank. Both pre- and post-monsoon data are included in this plot.

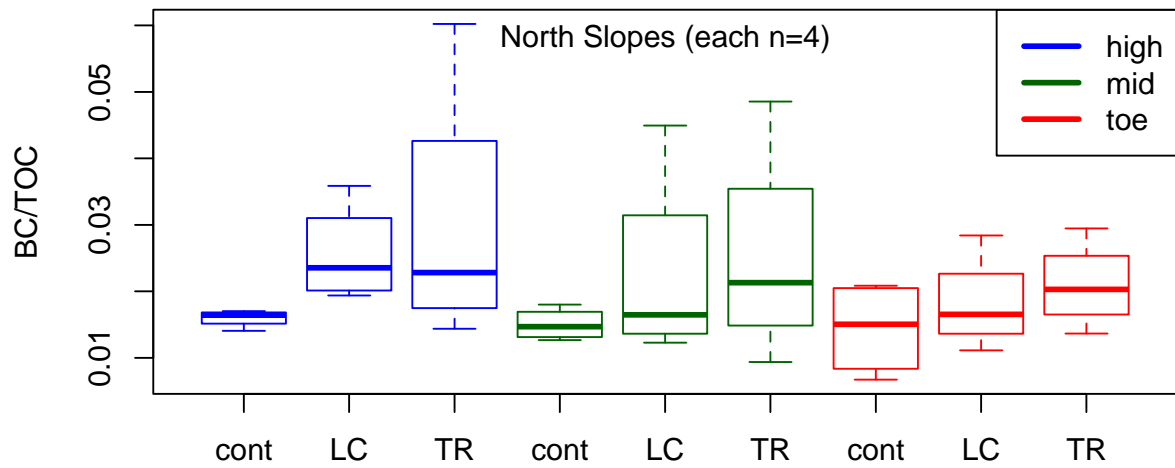


Figure 8. PyC soil content of north-facing hillslope sites stratified by longitudinal position on the hillslope. Both pre- and post-monsoon data are included in this plot.

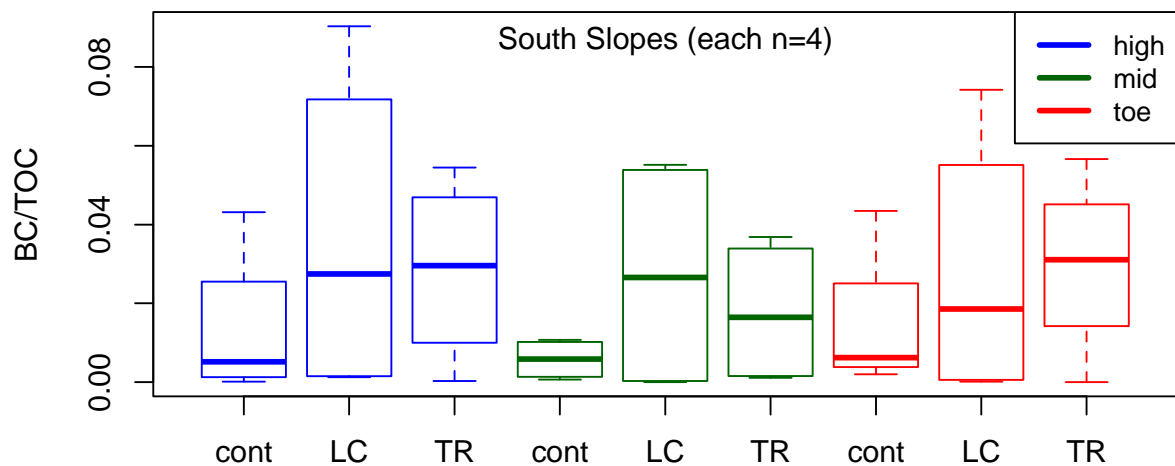


Figure 9. PyC soil content of south-facing hillslope sites stratified by longitudinal position on the hillslope. Both pre- and post-monsoon data are included in this plot.

The pre- and post-monsoon data is particularly important for quantifying redistribution of PyC by monsoonal rainfall events. The Thompson Ridge data for the sampled north-facing slope indicate a downslope transport of PyC during the monsoon, with concentrations near the summit declining and near the toe increasing from July to September 2013 (Figure 10). In contrast, the south-facing slope sampled in this area showed relatively constant BC content. The north slope had a slope of 16°, while the south facing slope had a slope of 30°. The Las Conchas and control slopes did not show a similar redistribution. The floodplain sampled downstream of the

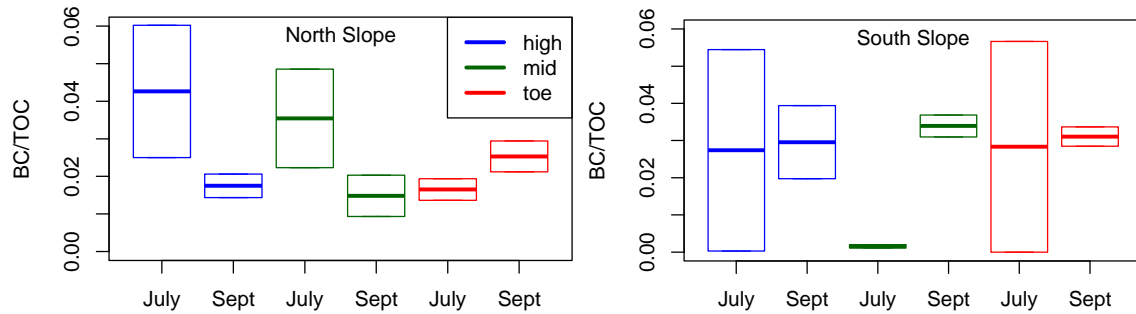


Figure 10. PyC soil content of the north- and south-facing hillslope sites in the Thompson Ridge burn area stratified by longitudinal position on the hillslope. July sample period was prior to most of the monsoon precipitation in 2013, while the September sample period followed the monsoon season.

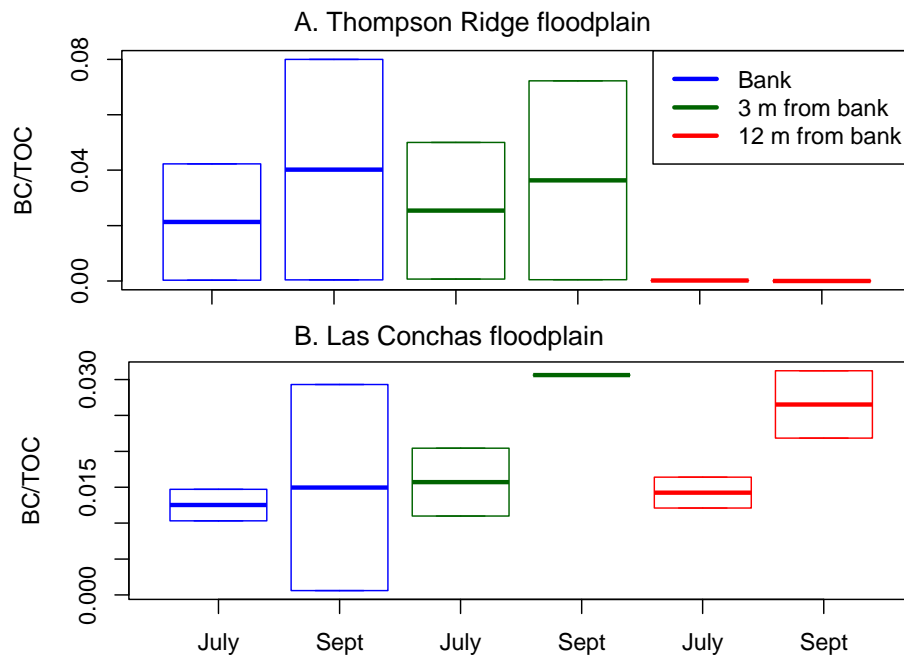


Figure 11. PyC soil content of the floodplain site, stratified by distance from the bank, in A) the Thompson Ridge burn area, and B) the Las Conchas burn area. July sample period was prior to most of the monsoon precipitation in 2013, while the September sample period followed the monsoon season. Sample sizes are  $n = 2$  for each box.



Thompson Ridge fire showed some evidence for accumulation of PyC during the monsoon flood season (Figure 11). None of these changes are significant due to the very small sample size ( $n=2$  for all comparisons of monsoon change data). Unfortunately, the post-monsoon fan samples have not yet been analyzed, precluding any major findings for alluvial fan dynamics at the single monsoon season time scale. Rather conclusions must be drawn by comparing the different times since burn at the three sampling sites.

### 3.3 Pre- and Post-Fire Soil Black Carbon Content

The resampled soil pit analysis yielded data on PyC content as a fraction of TOC for two soils depths, identified as the shallower “O” horizon and deeper “A” horizon, at two sampling times (2009 and 2014). PyC/TOC values for all samples ranged from 0.03 to 0.18 (Figure 12). The average O horizon concentration was 0.11 in 2009 and 0.10 in 2014, while the average A horizon concentration was 0.13 in 2009 and 0.12 in 2014 (Table 2). The O horizon had lower PyC concentration than the A horizon due to a larger mass of organic carbon, not a smaller mass of PyC. The three lowest PyC/TOC values were in post-fire O horizon soils that had TOC contents near the upper limit of the range of values observed combined with typical to slightly low PyC contents.

We investigated the carbon stock response of individual sites and soil horizons to the fire, finding seven samples with reduced PyC/TOC ratios, six samples with increased PyC/TOC ratios, and nine samples that were roughly unchanged (within 2% of the original value). Both O and A horizons gained and lost PyC with similar frequency (Figure 13), and in some cases the O horizon at a

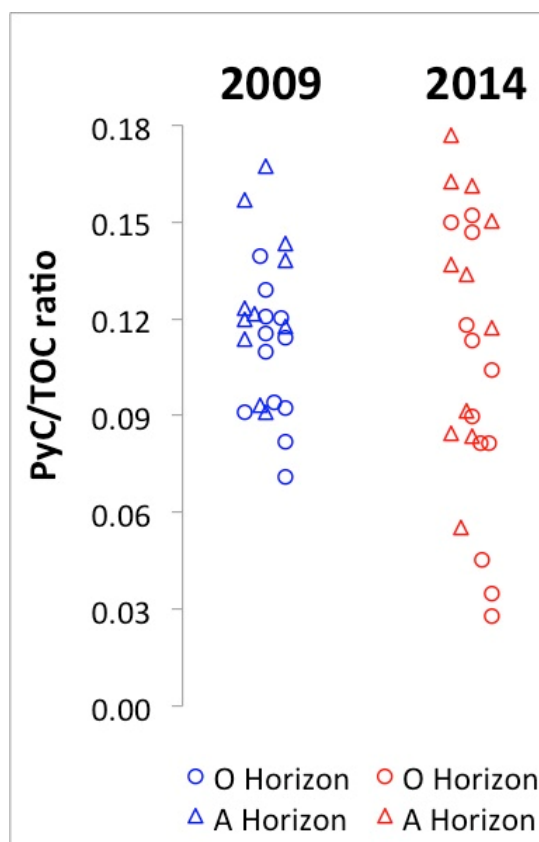


Figure 12. Pyrogenic black carbon (PyC) content as a fraction of total organic carbon (TOC) in soil samples from the Thompson Ridge burn taken before (2009) and after (2014) the fire. The “O” horizon was the upper 5 cm of soil if horization was not distinguishable following the fire.

single site gained PyC while the A horizon lost PyC, and vice versa. The PyC content, as a fraction of the soil mass, was more variable than the TOC content (Figure 14). In particular, PyC stocks in the O horizon changed dramatically from 2009 to 2014, with a nearly inverse relationship between values before and after the fire.

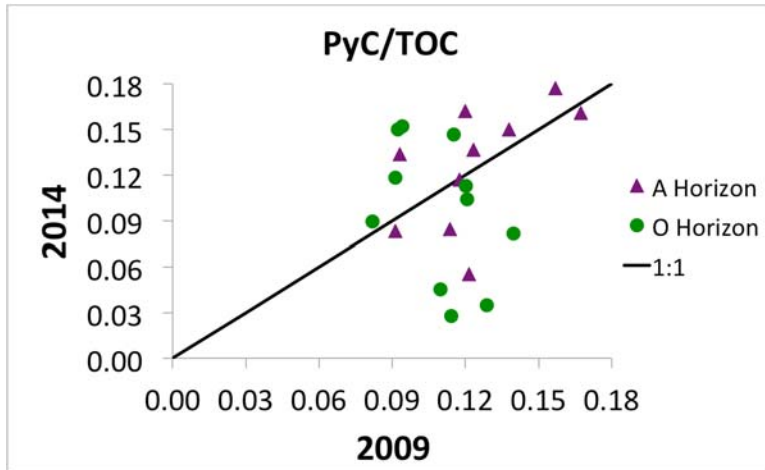


Figure 13. Temporal change in the ratio of pyrogenic black carbon to total organic carbon in soil pit samples. Points close to the 1:1 line were relatively unchanged in the Thompson Ridge fire. Point above the line gained black carbon, while points below the line lost black carbon.

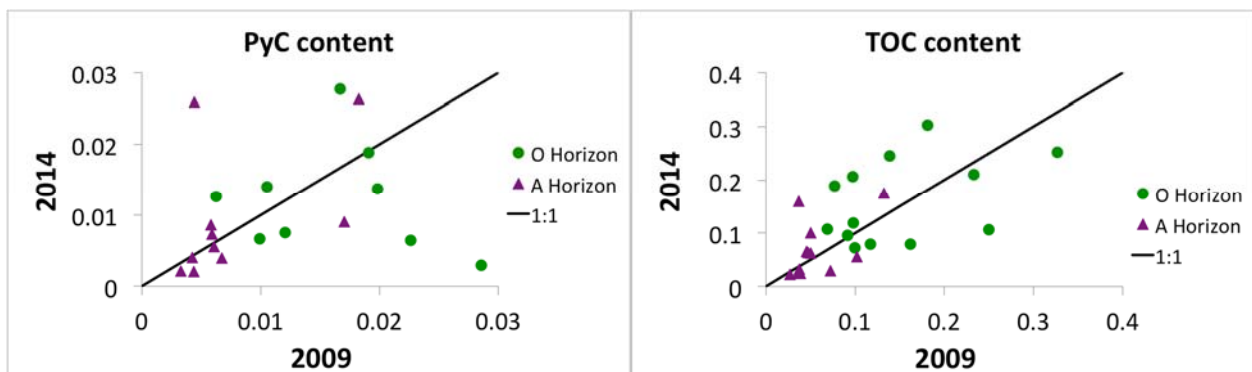


Figure 14. Temporal change in the pyrogenic black carbon content and the total organic carbon content in soil pit samples. Values are mass of PyC per unit mass of analyzed soil and mass of TOC per unit mass of soil. Soils were ground and sieved before analysis, removing any clasts larger than 250  $\mu\text{m}$ .

Table 2. Mean carbon stocks and ratios in pre- and post- fire soil pits

	Mean PyC content (mg/mg of soil)	Mean TOC content (mg/mg of soil)	Mean PyC/TOC ratio
O horizon 2009	0.016	0.149	0.11
O horizon 2014	0.016	0.159	0.10
A horizon 2009	0.008	0.056	0.13
A horizon 2014	0.009	0.068	0.12

To investigate possible controls on the gain and loss of PyC relative to TOC, we separated the sample sites into three groups corresponding to the watersheds of Redondo Creek, La Jara Creek, and Jaramillo Creek. We then sorted the sites from those nearest to the drainage divide to those nearest to the valley bottom or stream outlets. Figure 15 shows the three groups, separated again by O and A horizon. The A horizons are relatively stable, and do not show any distinguishable trends. The O horizons in all three watersheds show some degree of PyC loss in the upslope areas, and PyC gain in the downslope areas. This trend is variable and has some departures, as can be seen in the La Jara watershed data. It is most clearly shown in the Jaramillo watershed.

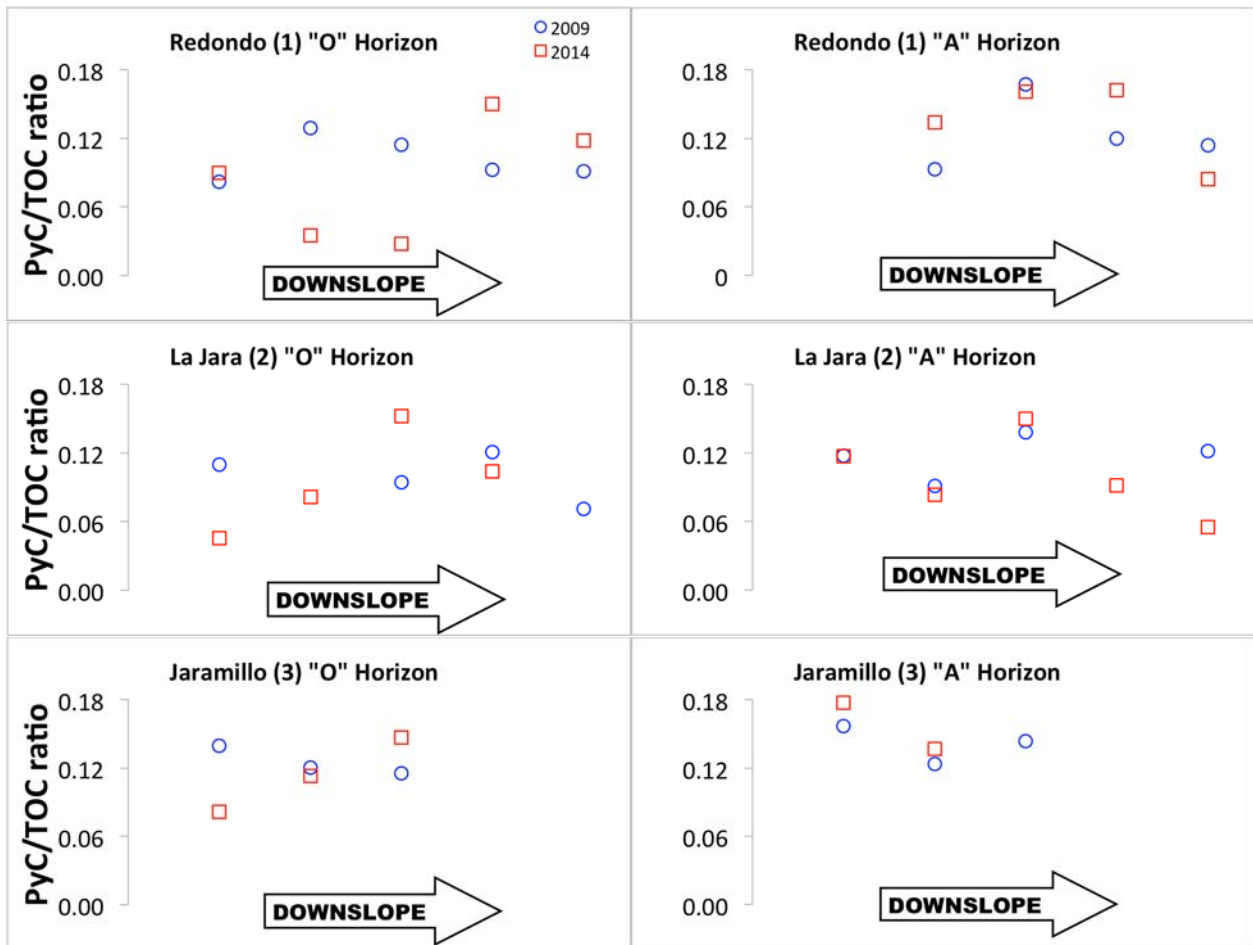


Figure 15. PyC/TOC ratio values of all analyzed sites, split by watershed group and soil horizon, then sorted into upslope (near the drainage divide) to downslope (near the watershed outlet) order. Blue circles are the 2009 data and red squares are the 2014 data. Note the relative stability of the A horizon samples. In some watersheds, the O horizon data show a trend toward PyC loss in the upslope areas and PyC gain in the downslope areas. Watershed group numbers correspond to numbers on the sample location map (Figure 3). Not all sampling locations had both O and A horizon data, or both 2009 and 2014 data, resulting in data gaps. For example, the upper-most site in the Redondo watershed did not have any A horizon data, and the lower-most site in the Jaramillo watershed did not have 2014 A horizon data.

### 3.4 Sorption of Arsenic onto Soils and Black Carbon

Batch experiments were conducted to examine sorption kinetics by extracting samples of the solution through time as the arsenic solution came into equilibrium with the soil. At very low concentrations, arsenic was released from the soil into the solution (Figure 16). This effect led to calculated “negative” sorption capacities, which made the 0.001 mg/L As solution data difficult to interpret. Presumably arsenic was also present on the soil in the other batch experiments, affecting the interpretation of the sorption capacities we calculated.

Four sorbents were tested: a hillslope soil, a floodplain soil, a floodplain soil to which field collected char had been added to increase PyC content by 4% of the soil mass, and activated charcoal. The results of the activated charcoal batches are not readily interpreted. There may have been undetected instrument error when these samples were analyzed. Due to the uncertainty associated with these data, they will not be further analyzed in this report, but the data are presented for completeness.

At solute concentrations of 0.005 mg/L, sorption kinetics were nearly indistinguishable among the three soils (Figure 17). The curves were well fit by a pseudo-second order kinetic equation of the form

$$q_t = \frac{tkq_e^2}{(1+tkq_e)} \quad \text{Eq. 1}$$

where  $t$  is time (hr),  $q_t$  is the amount sorbed at time  $t$  per unit mass of soil ( $\text{mg g}^{-1}$ ),  $q_e$  is the amount sorbed at equilibrium ( $\text{mg g}^{-1}$ ), and  $k$  is the equilibrium rate constant of sorption ( $\text{g mg}^{-1} \text{hr}^{-1}$ ) (Ho and McKay, 1999). Eq. 1 can be reformulated as

$$\frac{t}{q_t} = \frac{1}{q_e}t + \frac{1}{kq_e^2} \quad \text{Eq. 2}$$

for simple linear parameter fitting in the  $t$  vs.  $t/q_t$  parameter space.

At solute concentrations of 0.01 mg/L, the two natural soils still showed strongly similar sorption kinetics, but the soil augmented with PyC had a slightly higher equilibrium sorption capacity (Figure 18). At solute concentrations of 0.1 mg/L, the floodplain soil is beginning to show slightly higher sorption capacity than the hillslope soil, and the difference in the soil augmented

with PyC is becoming pronounced (Figure 19). The early time sorption onto the PyC augmented soil is particularly enhanced, with a maximum difference at about 3 hours.

For a given soil, the equilibrium sorption capacity in the presence of the 0.01 mg/L arsenic solution was roughly 2.3 times the capacity in the presence of the 0.005 mg/L (Figure 20). Likewise, for the same soil, the equilibrium sorption capacity in the presence of the 0.1 mg/L arsenic solution was roughly 13 times the capacity in the presence of the 0.01 mg/L. Thus there is a ~2.3 fold increase in sorption for a 2-fold increase in arsenic concentration, and a 13-fold increase in sorption for a 10-fold increase in arsenic concentration.

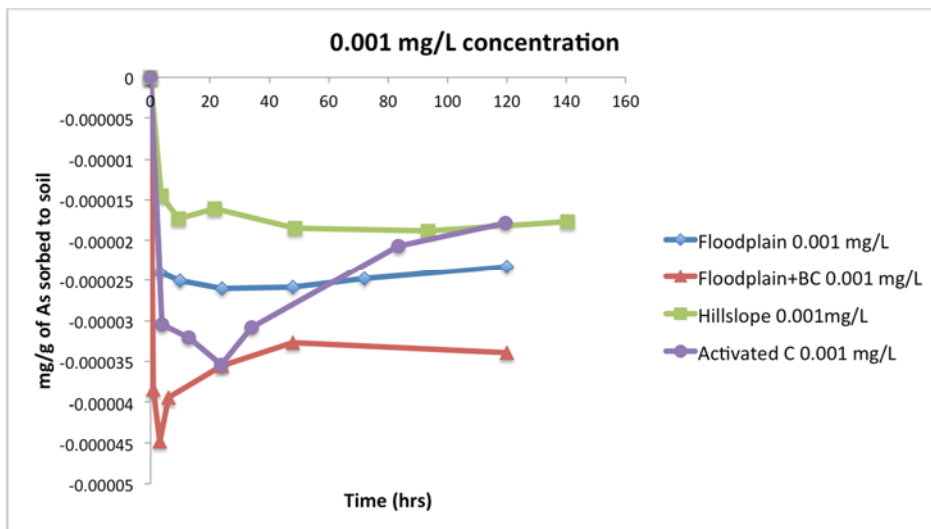


Figure 16. Sorption kinetics for 0.001 mg/L As solution.

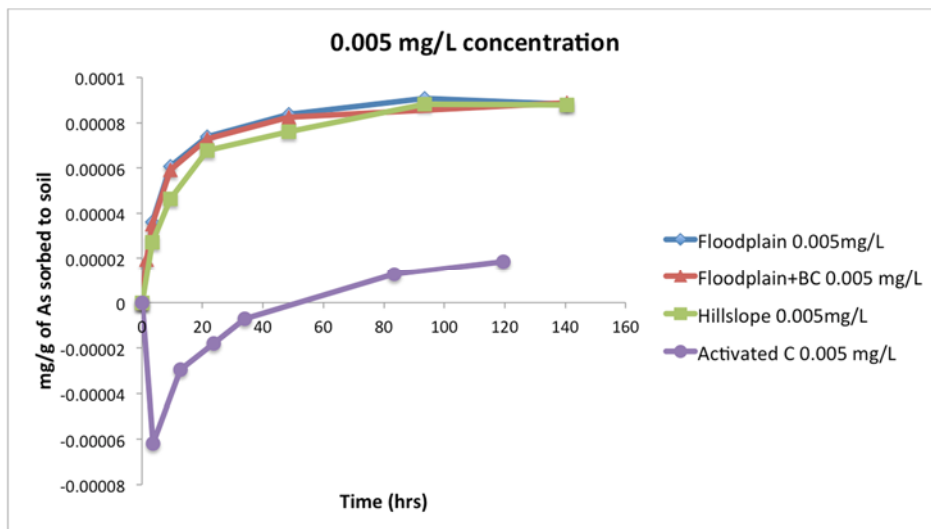


Figure 17. Sorption kinetics for 0.005 mg/L As solution.

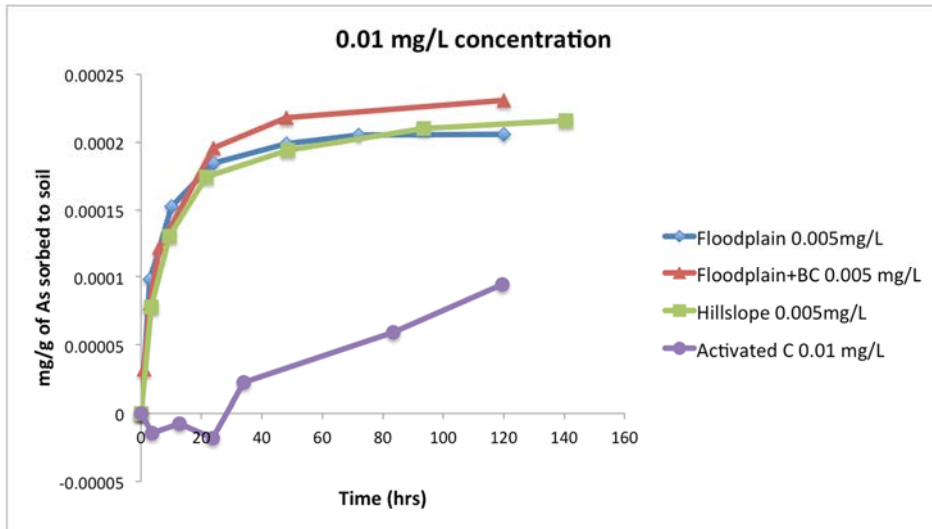


Figure 18. Sorption kinetics for 0.01 mg/L As solution.

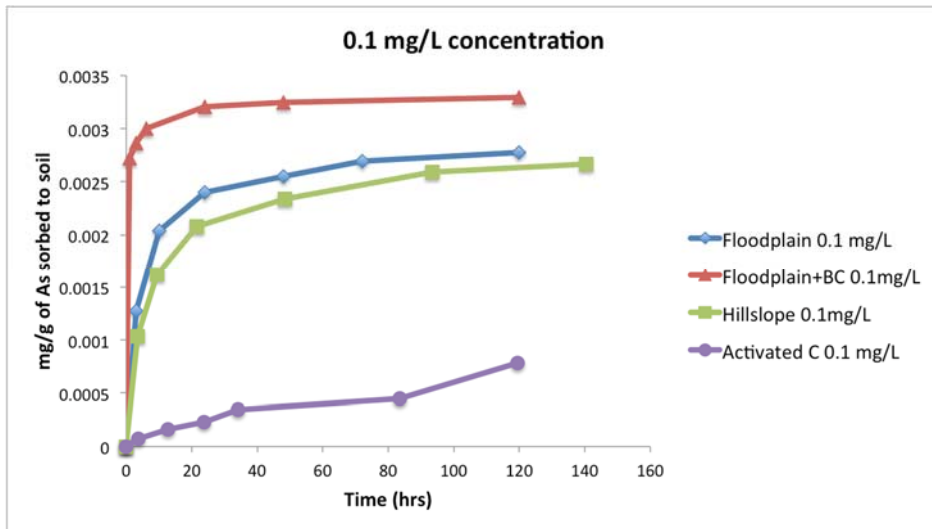


Figure 19. Sorption kinetics for 0.1 mg/L As solution.

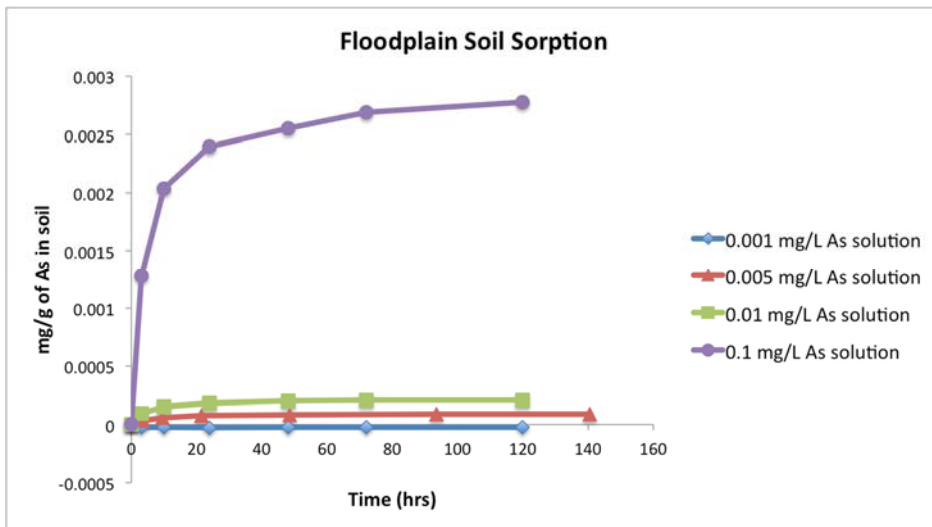


Figure 20. Sorption kinetics on the floodplain soil for all four As solutions.

The equilibrium isotherms from the replicate batches matched well with the final equilibrium data from the kinetic experiments for the floodplain soil, but less so for the hillslope soil (Figure 21), and for the PyC augmented floodplain soil the data appear to be unreliable and are not presented. The linear trend on the logarithmic plot gives a good fit to the Freundlich isotherm, but this equation is empirical and meaning is difficult to assign. The data fit extremely poorly with the Langmuir isotherm equation. In a Langmuir isotherm situation, you would expect a doubling of concentration to lead to less than a doubling of sorption, while we observed more than a doubling. The data fit well to a Dubinin-Radushkevich isotherm, given by the equation

$$q_e = q_d \exp\left(-B_d \left[RT \ln\left(1 + \frac{1}{C_e}\right)\right]^2\right) \quad \text{Eq. 3}$$

where  $q_e$  is the solid phase arsenic concentration at equilibrium (mg/g),  $C_e$  is the liquid phase arsenic concentration at equilibrium (mg/L),  $q_d$  is a constant (mg/g), and  $B_d$  is also a constant (unitless). The Dubinin-Radushkevich isotherm theoretically describes diffusion into the heterogeneous pore structure of the sorbent.

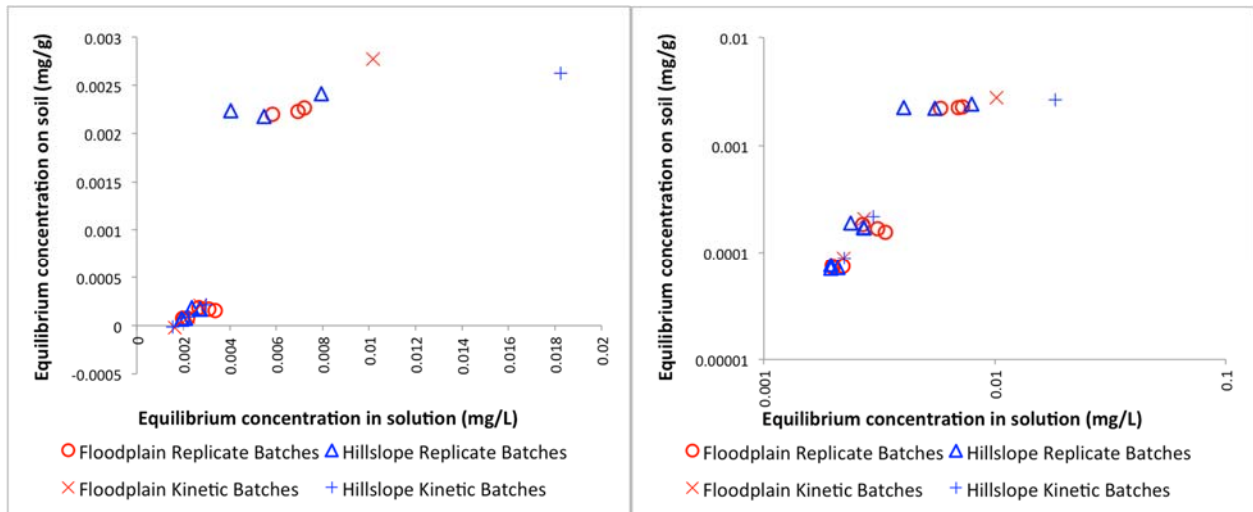


Figure 21. Equilibrium isotherms for arsenic sorption to the floodplain and hillslope soils. The left figure has a linear scale, while the right figure has a logarithmic scale.

The pH and oxidation-reduction potential (redox potential, ORP) of each solution was measured at the end of each equilibration. Both pH and ORP will affect the speciation of As and thus its

sorption characteristics. In our experiments, the pH and ORP values suggest that As was present as As(V) arsenate (Masscheleyn et al. 1991, Figure 22). In particular, the experiments were conducted in oxidizing conditions, similar to the expected conditions in the vadose zone. Below the water table, reducing conditions could promote conversion of As(V) to As(III), which will have different sorption characteristics. According to the As-H<sub>2</sub>O system diagram of Masscheleyn et al. (1991) our experimental conditions would consistently promote As(V), however the pH changed enough that the degree of protonation may vary between our experimental runs (Figure 22). The floodplain soil and floodplain soil mixed with additional black carbon both have higher pH values that suggest the predominance of HAsO<sub>4</sub><sup>2-</sup> (Figure 22), which would sorb less easily to negatively charged surfaces than the H<sub>2</sub>AsO<sub>4</sub><sup>-</sup> that is expected to predominate in our hillslope and field char experimental conditions. The pH trends with increasing As concentration are not consistent between sorbents, and show no trend with some sorbents (Figure 23).

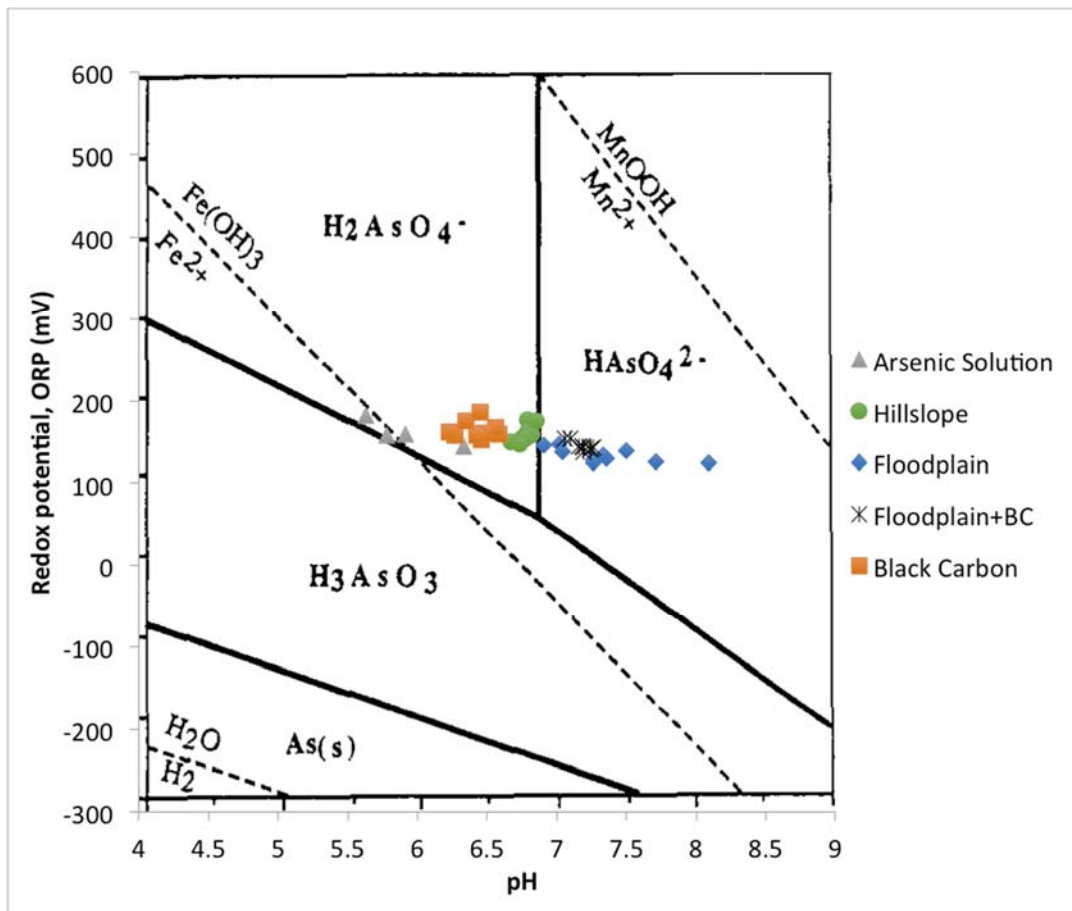


Figure 22. ORP and pH data of equilibrated sorbent-sorbate systems plotted on an Eh-pH diagram for the As-H<sub>2</sub>O system, from Masscheleyn et al. 1991. Activities of As, Mn, and Fe were all taken to be 10<sup>-4</sup>. Species areas indicated are ‘predominance areas’, not strict limits for existence.



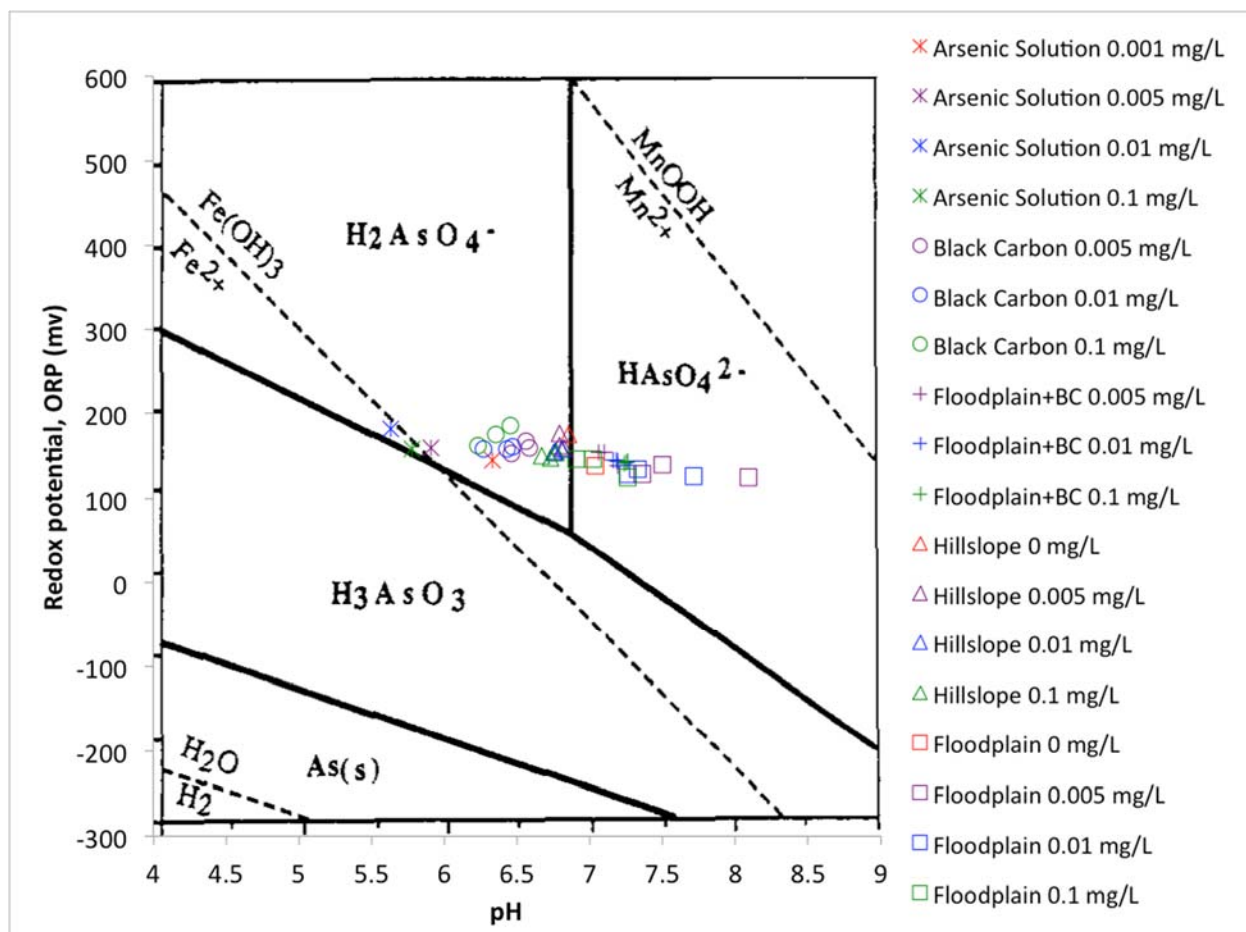


Figure 23. Same Eh-pH diagram as Figure 21, from Masscheleyn et al. 1991, with sample pH and ORP separated according to the concentration of As sorbate solution.

## 4. DISCUSSION

### 4.1 Black Carbon Distribution

Our broad-scale results only enable discussion of soot particles, which may travel large distances before deposition. In spite of this potential for widespread transport, there appears to be evidence for enhanced local deposition following fires. The Thompson Ridge burn area had the greatest PyC content detected by our analysis, and was also the site of the most recent fire. There is also evidence that following fire inputs, the soot content of soils decreases. This may be due to dissolution, biochemical breakdown, or erosion and downstream transport.

Soil texture did not appear to have a consistent affect on the results of either the landscape scale sampling or the pre- and post-fire sampling. The sites did cross a range of soils and soil textures

(Figure 2), although they were predominantly sandy loams with varying amounts of gravel and cobbles. Soils in the study area are formed on volcanic debris that has a broad grain size distribution. Clay-sized particles were universally present, so the contribution of clay minerals to sorption is likely to be substantial.

#### **4.2 Black Carbon Generation and Retention**

Our pre-fire/post-fire soil pit comparison showed little change in mean PyC content averaged over all sampling sites, either as a fraction of total soil analyzed or as a fraction of TOC. This surprising result may be due to the delay in post-fire sampling; perhaps there was a temporary increase in PyC immediately after the fire, but subsequent storms prior to our sampling may have removed it. Another possible mechanism of PyC removal is the combustion of soil PyC reservoirs during the fire itself. It is possible that temperatures during the fire are hot enough to oxidize the soil PyC into CO<sub>2</sub>, with the stores then being replaced with partially combusted organic matter from the later stages of the fire. This would only need to be invoked for the O horizon, since the A horizon is presumably both shielded from the heat and unable to receive new PyC, easily explaining the stability of the PyC content at this deeper position. Finally, it is possible that PyC stores did in fact increase, but that the increase was dominated by poorly condensed chars that were eliminated in the 340 °C combustion we used to remove organic carbon.

Although we cannot eliminate any of these explanations – post-fire erosion of PyC, combustion of PyC during the fire, or dominance of unquantified char – as causes for the stability of pre- and post-fire soil PyC content, there is some evidence in favor of post-fire erosion as being an important contributor. The average values were stable, but local sites did show changes in PyC content, especially in the O horizon. The trend of PyC loss in steep, upslope, and more intensely burned areas combined with PyC increases in flat, downslope, or riparian areas suggest that PyC was eroded from hillslopes and re-deposited further down-gradient. This conclusion from the pre- and post-fire soil pit data also finds some support in the broad-scale data, discussed in the next section.

### 4.3 Black Carbon Transport

Transport of PyC, as measured by pre- and post-monsoon differences in content, show a downslope transport of PyC on the north slope sampled in the Thompson Ridge burn area, but no transport on the more steeply sloping south hillslope we sampled. The increase of PyC near the channel downstream of this area, but isolated to the areas where evidence of flooding was observed, suggest that floodwaters transport PyC and deposit at least some of it on the floodplain. The continued high PyC content in floodplain soils downstream of the Las Conchas fire (Figure 3), and the observed increase in PyC content in this area during the 2013 monsoon (Figure 9B), suggest that this process may continue for several years following a fire. There was a moderately high concentration of PyC on the Thompson Ridge alluvial fan that we sampled, but very little on the fans in the control and Las Conchas areas. We have not yet analyzed the post-monsoon samples to determine if it remained in place, gained new PyC, or eroded away. Nevertheless, it appears that if soot is stored on fans it is for a relatively short period when compared to floodplains and even hillslopes. Debris flow deposits were observed in areas affected by the Las Conchas fire, but not in the Thompson Ridge area. This suggests that such high-energy events, while clearly important for fan building, tend to transport most PyC to more distal locations.

The levels of soot PyC in the control catchment, while less than those in the recently burned catchments by about 40%, were still substantial. This could either be an indicator of the recalcitrance of black carbon (e.g., Cheng et al., 2008), or it could reflect distal deposition of windblown ash mobilized during nearby fires or in post-fire wind events (Whicker et al, 2006). Indeed, even transport within the watershed is likely to represent a combination of aeolian and fluvial processes, although the floodplain transects suggest fluvial transport is the dominant mode.

For these reasons we conclude that runoff and flood transport is more important to soot and ash dynamics than debris flow transport, at least at our sampled locations. This conclusion is consistent with prior observations of anoxic zones that developed downstream of the Las Conchas burn during floods immediately after the fire (David Van Horn, UNM, personal communication). Likewise, black, tar-like river flows were observed in the Cache la Poudre

River near Fort Collins, CO during the first rainstorm following the High Park fire in June 2012 (Ellen Wohl, CSU, personal communication). Our analysis using the CTO-375 method does not permit us to draw any conclusions regarding the transport or retention of char.

#### **4.4 Post-Fire Debris Management Implications**

If most soot and ash is transported in floods over several years following fire, the duration of downstream impact should be relatively limited. The first monsoon season following a fire will be the primary event for which mitigation plans need to be prepared, at least from the perspective of soot alone. Background soil soot content was significantly lower in the control site, but still at a level that suggests a significant portion of the deposition is quite recalcitrant and may impact soil water chemistry for decades. The full impact of PyC is difficult to evaluate, because of the range of materials encompassed by the term and the difficulty of completely measuring the full range. Likewise, the rapid transport and redeposition following fire documented here suggest that spatial variability will be high and the impact will vary over short distances.

#### **4.5 Potential to Sequester Arsenic**

The arsenic sorption characteristics of the soils collected in Valles Caldera did not vary greatly between hillslope and floodplain soils. More surprisingly, the addition of activated carbon did not significantly increase equilibrium sorption capacity of the floodplain soil for low concentrations of As. It did, however, increase the sorption capacity of the soil when exposed to high concentrations of As. The effect was particularly strong in the first few hours of exposure. The difference between the unaltered soil and the activated charcoal augmented soil diminished somewhat as the batches approached equilibrium. The good fit of the Dubinin-Radushkevich isotherm equation, along with the limited impact of PyC augmentation, suggests that the soils of Valles Caldera are quite capable of sorbing environmentally significant concentrations of arsenic due to their physical structure and abundance of clays. However, if a contaminant that behaves similarly to arsenic is released as a highly concentrated and mobile plume, PyC content will have an increasingly significant effect on its mobility. But for low, chronic concentrations of arsenic that permit long equilibration times, PyC augmentation would have limited effectiveness in increasing sequestration potential.

#### **4.6 Ongoing and Future Work**

Work is ongoing on several aspects of this project, funded by a National Science Foundation grant that is a follow-on to the New Mexico Water Resources Research Institute seed grant reported on here. The remaining landscape-scale samples will be analyzed for PyC content, and the trends observed in the analysis of the partial set will be either confirmed or modified. The qualitative spatial trends in PyC gain or loss following fire reported here will be investigated quantitatively using a GIS. We are also exploring ways to make the PyC concentrations found using the modified CTO method more comparable with other quantification approaches, such as BPCA analysis. Chromium sorption experiments will be conducted for comparison with the arsenic experiments. The potential influence of pH and redox potential on our sorption results will be explored in greater detail. And finally, we plan to test the capacity of our soils to sorb an aromatic hydrocarbon such as benzene as a representative organic contaminant.

## 5. REFERENCES

- Accardi-Dey, A. and Gschwend, P.M. (2003) Reinterpreting literature sorption data considering both absorption into organic carbon and adsorption onto black carbon. *Environmental Science & Technology* 37(1), 99-106.
- Arp, H.P.H., Breedveld, G.D. and Cornelissen, G. (2009) Estimating the in situ sediment-porewater distribution of PAHs and chlorinated aromatic hydrocarbons in anthropogenic impacted sediments. *Environmental Science & Technology* 43(15), 5576-5585.
- Bailey, S.E., Olin, T.J., Bricka, R.M. and Adrian, D.D. (1999) A review of potentially low-cost sorbents for heavy metals. *Water Research* 33(11), 2469-2479.
- Brodowski, S., Rodionov, A., Haumaier, L., Glaser, B. and Amelung, W. (2005) Revised black carbon assessment using benzene polycarboxylic acids. *Organic Geochemistry* 36(9), 1299-1310.
- Caria, G., Arrouays, D., Dubromel, E., Jolivet, C., Ratié, C., Bernoux, M., Barthès, B.G., Brunet, D. and Grinand, C. (2011) Black carbon estimation in French calcareous soils using chemo-thermal oxidation method. *Soil Use and Management* 27(3), 333-339.
- Certini, G. (2005) Effects of fire on properties of forest soils: a review. *Oecologia* 143(1), 1-10.
- Chen, J., Zhu, D. and Sun, C. (2007) Effect of heavy metals on the sorption of hydrophobic organic compounds to wood charcoal. *Environmental Science & Technology* 41(7), 2536-2541.
- Cheng, C.-H., Lehmann, J., Thies, J.E. and Burton, S.D. (2008) Stability of black carbon in soils across a climatic gradient. *J. Geophys. Res.* 113(G2), G02027.
- Chorover, J., Troch, P.A., Rasmussen, C., Brooks, P.D., Pelletier, J.D., Breshears, D.D., Huxman, T.E., Kurc, S.A., Lohse, K.A., McIntosh, J.C., Meixner, T., Schaap, M.G., Litvak, M.E., Perdrial, J., Harpold, A. and Durcik, M. (2011) How water, carbon, and energy drive critical zone evolution: The Jemez-Santa Catalina Critical Zone Observatory. *Vadose Zone Journal* 10(3), 884-899.
- Cornelissen, G., Gustafsson, Ö., Bucheli, T.D., Jonker, M.T.O., Koelmans, A.A. and van Noort, P.C.M. (2005) Extensive sorption of organic compounds to black carbon, coal, and kerogen in sediments and soils: Mechanisms and consequences for distribution, bioaccumulation, and biodegradation. *Environmental Science & Technology* 39(18), 6881-6895.
- Czimczik, C.I. and Masiello, C.A. (2007) Controls on black carbon storage in soils. *Global Biogeochem. Cycles* 21(3), GB3005.
- Czimczik, C.I., Preston, C.M., Schmidt, M.W.I. and Schulze, E.-D. (2003) How surface fire in Siberian Scots pine forests affects soil organic carbon in the forest floor: Stocks, molecular structure, and conversion to black carbon (charcoal). *Global Biogeochem. Cycles* 17(1), 1020.
- DeLuca, T.H., MacKenzie, M.D., Gundale, M.J. and Holben, W.E. (2006) Wildfire-produced charcoal directly influences nitrogen cycling in ponderosa pine forests. *Soil Sci. Soc. Am. J.* 70(2), 448-453.
- Dillon, G.K., Holden, Z.A., Morgan, P., Crimmins, M.A., Heyerdahl, E.K. and Luce, C.H. (2011) Both topography and climate affected forest and woodland burn severity in two regions of the western US, 1984 to 2006. *Ecosphere* 2(12), art130.
- Dittmar, T. (2008) The molecular level determination of black carbon in marine dissolved organic matter. *Organic Geochemistry* 39(4), 396-407.
- Eckmeier, E., Gerlach, R., Skjemstad, J., Ehrmann, O. and Schmidt, M. (2007) Minor changes in soil organic carbon and charcoal concentrations detected in a temperate deciduous forest a year after an experimental slash-and-burn. *Biogeosciences* 4, 377-383.
- Elmqvist, M., Gustafsson, Ö. and Andersson, P. (2004) Quantification of sedimentary black carbon using the chemothermal oxidation method: an evaluation of ex situ pretreatments and standard additions approaches. *Limnology and Oceanography: Methods* 2(12), 417-427.
- Forbes, M.S., Raison, R.J. and Skjemstad, J.O. (2006) Formation, transformation and transport of black carbon (charcoal) in terrestrial and aquatic ecosystems. *Science of The Total Environment* 370(1), 190-206.
- Ghosh, U. (2007) The role of black carbon in influencing availability of PAHs in sediments. *Human and Ecological Risk Assessment: An International Journal* 13(2), 276-285.

- Goldberg, E.D. (1985) *Black Carbon in the Environment: Properties and Distribution*, John Wiley & Sons, New York.
- Gundale, M. and DeLuca, T. (2007) Charcoal effects on soil solution chemistry and growth of *Koeleria macrantha* in the ponderosa pine/Douglas-fir ecosystem. *Biology and Fertility of Soils* 43(3), 303-311.
- Gustafsson, Ö., Bucheli, T.D., Kukulska, Z., Andersson, M., Largeau, C., Rouzaud, J.-N., Reddy, C.M. and Eglinton, T.I. (2001) Evaluation of a protocol for the quantification of black carbon in sediments. *Global Biogeochemical Cycles* 15(4), 881-890.
- Gustafsson, Ö., Haghseta, F., Chan, C., MacFarlane, J. and Gschwend, P.M. (1997) Quantification of the dilute sedimentary soot phase: Implications for PAH speciation and bioavailability. *Environmental Science & Technology* 31(1), 203-209.
- Hammes, K., Schmidt, M.W.I., Smernik, R.J., Currie, L.A., Ball, W.P., Nguyen, T.H., Louchouart, P., Houel, S., Gustafsson, O. and Elmquist, M. (2007) Comparison of quantification methods to measure fire-derived (black/elemental) carbon in soils and sediments using reference materials from soil, water, sediment and the atmosphere. *Global Biogeochemical Cycles* 21(3), GB3016.
- Hammes, K., Torn, M., Lapenas, A. and Schmidt, M. (2008) Centennial black carbon turnover observed in a Russian steppe soil. *Biogeosciences* 5, 1339-1350.
- Ho, Y.S. and McKay, G. (1999) A kinetic study of dye sorption by biosorbent waste product pith. *Resources, Conservation and Recycling* 25(3-4), 171-193.
- Hockaday, W.C., Grannas, A.M., Kim, S. and Hatcher, P.G. (2006) Direct molecular evidence for the degradation and mobility of black carbon in soils from ultrahigh-resolution mass spectral analysis of dissolved organic matter from a fire-impacted forest soil. *Organic Geochemistry* 37(4), 501-510.
- Incident Information System (IIS), (2013) Thompson Ridge Fire. <http://inciweb.nwcg.gov/incident/3404/>
- Jaffé, R., Ding, Y., Niggemann, J., Vähätalo, A.V., Stubbins, A., Spencer, R.G.M., Campbell, J. and Dittmar, T. (2013) Global charcoal mobilization from soils via dissolution and riverine transport to the oceans. *Science* 340(6130), 345-347.
- Kim, S., Kaplan, L.A., Benner, R. and Hatcher, P.G. (2004) Hydrogen-deficient molecules in natural riverine water samples—evidence for the existence of black carbon in DOM. *Marine Chemistry* 92(1-4), 225-234.
- Koelmans, A.A., Jonker, M.T.O., Cornelissen, G., Bucheli, T.D., Van Noort, P.C.M. and Gustafsson, Ö. (2006) Black carbon: The reverse of its dark side. *Chemosphere* 63(3), 365-377.
- Kuhlbusch, T.A.J. (1995) Method for determining black carbon in residues of vegetation fires. *Environmental Science & Technology* 29(10), 2695-2702.
- Lehmann, J. (2007) Bio-energy in the black. *Frontiers in Ecology and the Environment* 5(7), 381-387.
- Lehmann, J., Pereira da Silva, J., Jr., Steiner, C., Nehls, T., Zech, W. and Glaser, B. (2003) Nutrient availability and leaching in an archaeological Anthrosol and a Ferralsol of the Central Amazon basin: fertilizer, manure and charcoal amendments. *Plant and Soil* 249(2), 343-357.
- Liang, B., Lehmann, J., Solomon, D., Kinyangi, J., Grossman, J., O'Neill, B., Skjemstad, J.O., Thies, J., Luizão, F.J., Petersen, J. and Neves, E.G. (2006) Black carbon increases cation exchange capacity in soils. *Soil Sci. Soc. Am. J.* 70(5), 1719-1730.
- Liang, B., Lehmann, J., Solomon, D., Sohi, S., Thies, J.E., Skjemstad, J.O., Luizão, F.J., Engelhard, M.H., Neves, E.G. and Wirrick, S. (2008) Stability of biomass-derived black carbon in soils. *Geochimica et Cosmochimica Acta* 72(24), 6069-6078.
- Litschert, S.E., Brown, T.C. and Theobald, D.M. (2012) Historic and future extent of wildfires in the Southern Rockies Ecoregion, USA. *Forest Ecology and Management* 269(0), 124-133.
- Masiello, C.A. (2004) New directions in black carbon organic geochemistry. *Marine Chemistry* 92(1-4), 201-213.
- Masscheleyn, P.H., Delaune, R.D. and Patrick, W.H. (1991) Effect of redox potential and pH on arsenic speciation and solubility in a contaminated soil. *Environmental Science & Technology* 25(8), 1414-1419.
- Nguyen, B., Lehmann, J., Kinyangi, J., Smernik, R., Riha, S. and Engelhard, M. (2008) Long-term black carbon dynamics in cultivated soil. *Biogeochemistry* 92(1-2), 163-176.

- Nguyen, T.H., Brown, R.A. and Ball, W.P. (2004) An evaluation of thermal resistance as a measure of black carbon content in diesel soot, wood char, and sediment. *Organic Geochemistry* 35(3), 217-234.
- Ohlson, M., Dahlberg, B., Okland, T., Brown, K.J. and Halvorsen, R. (2009) The charcoal carbon pool in boreal forest soils. *Nature Geoscience* 2(10), 692-695.
- Qiu, Y., Cheng, H., Xu, C. and Sheng, G.D. (2008) Surface characteristics of crop-residue-derived black carbon and lead(II) adsorption. *Water Research* 42(3), 567-574.
- Schmidt, M.W.I. and Noack, A.G. (2000) Black carbon in soils and sediments: Analysis, distribution, implications, and current challenges. *Global Biogeochem. Cycles* 14(3), 777-793.
- Schumacher, B.A., 2002. Methods for the determination of total organic carbon (TOC) in soils and sediments. United States Environmental Protection Agency, NCEA-C-1282.
- Smith, H.G., Sheridan, G.J., Lane, P.N.J., Nyman, P. and Haydon, S. (2011) Wildfire effects on water quality in forest catchments: A review with implications for water supply. *Journal of Hydrology* 396(1-2), 170-192.
- Southwest Coordination Center (SWCC), (2012) Las Conchas Fire, Jemez NM. [http://swfireconsortium.org/wp-content/uploads/2012/11/Las-Conchas-Factsheet\\_bsw.pdf](http://swfireconsortium.org/wp-content/uploads/2012/11/Las-Conchas-Factsheet_bsw.pdf)
- Staniszewska, M., Burska, D., Sapota, G., Bogdaniuk, M., Borowiec, K., Nosarzewska, I. and Bolalek, J. (2011) The relationship between the concentrations and distribution of organic pollutants and black carbon content in benthic sediments in the Gulf of Gdańsk, Baltic Sea. *Marine Pollution Bulletin* 62(7), 1464-1475.
- Wang, X.S., Chen, L.F., Li, F.Y., Chen, K.L., Wan, W.Y. and Tang, Y.J. (2010) Removal of Cr (VI) with wheat-residue derived black carbon: Reaction mechanism and adsorption performance. *Journal of Hazardous Materials* 175(1-3), 816-822.
- Whicker, J.J., Pinder, J.E. and Breshears, D.D. (2006) Increased Wind Erosion from Forest Wildfire: Implications for Contaminant-Related Risks. *Journal of Environmental Quality* 35(2), 468-478.
- Wiedemeier, D.B., Hilf, M.D., Smittenberg, R.H., Haberle, S.G. and Schmidt, M.W.I. (2013) Improved assessment of pyrogenic carbon quantity and quality in environmental samples by high-performance liquid chromatography. *Journal of Chromatography A* 1304(0), 246-250.